University of Natural Resources and Life Sciences, Vienna

Department of Agrobiotechnology, IFA-Tulln

Institute of Biotechnology in Plant Production

Fine Mapping of the Fusarium Head Blight Resistance QTL *Qfhs.ifa-5*A through Radiation Induced Deletion Mapping of a Gamma Treated Wheat Population

Master Thesis submitted by:

Petra Schwarz

01340503

Supervisors:

Univ.-Prof. Dipl.-Ing. Dr. nat. techn. Hermann Bürstmayr

Dipl.-Ing. Maria Bürstmayr

Dipl.-Ing. Dr. Barbara Steiner

ACKNOWLEDGEMENTS

Foremost I would like to express my deepest gratitude to my supervisors, prof. Hermann Bürstmayr, Dr. Barbara Steiner, and Dipl.-Ing. Maria Bürstmayr for their support during this project.

Special thanks to Maria Bürstmayr, for her guidance, constructive comments, and endless patience. Thank you for everything you have taught me, and for always being there for me.

I wish to thank all my colleagues at IFA-Tulln, especially Simone Zimmerl and Christian Wagner, for all the help and advices they have provided. It was always a pleasure working with such lovely and engaging people.

Last but not least, to the one who encourages me to follow my dreams. My greatest support, my husband Matthias, thank you for your unconditional love and motivation.

This research was part of the project SFB F3711-B05, supported by the Austrian Science Fund (FWF).

ABSTRACT

Fusarium head blight (FHB) is a fungal disease of small grain cereals affecting yield and grain quality. One major quantitative trait loci (QTL) for FHB resistance in wheat is *Qfhs.ifa-5A*, located on the 5A chromosome. Genetic map from earlier molecular analysis confined the QTL between the flanking markers *barc186* and *barc180*, spreading across the centromere. Genetic maps are based on recombination frequency, which is influenced by chromosome structure. Reduced recombination rate around centromere aggravates fine mapping of the pericentromeric region. Additionally, the necessity of polymorphic markers drastically reduces number of markers that could be used for mapping. To overcome the difficulties posed by genetic mapping, alternative approach was used to obtain a high-resolution map of the *Qfhs.ifa-5A* supporting interval. Radiation causes chromosomal breakages that can, via error prone repair mechanism, lead to deletions. These artificially induced deletions are random across the genome and recombination independent. Moreover, induced deletion mapping is based on presence or absence of marker loci, allowing to map monomorphic markers, as well. Two different panels were used in this study. Radiation induced deletion panel (Del-NIL3) was created by irradiating seeds of a near-isogenic line carrying *Qfhs.ifa-5A*, followed by self-pollination. Chinese Spring radiation hybrid (CS-RH) was obtained by irradiating pollen of Chinese Spring and pollinating an aneuploid line of Chinese Spring missing the 5A chromosome. Overall, 1764 Del-NIL3 and 276 CS-RH lines were genotyped with 35 molecular markers. Results of both panels positioned nine molecular markers in the bin farthest from the centromere, 5AS3-0.75-0.97, 13 markers in the 5AS1-0.40-0.75, and 13 in the bin closest to the centromere C-5AS1-0.40. CS-RH lines demonstrated higher number of deletion lines, with almost two-fold longer deletions in physical size, nevertheless the seed irradiated panel provided better resolution. Consensus map derived from 28 Del-NIL3 and 40 CS-RH informative lines covered the distance of 324.8 cR, with resolution of 0.88 Mbp/cR. Consensus map based on radiation induced deletions had 253-fold increased resolution than genetic map for the *barc186* and *cfa2250* region. This striking improvement in map resolution indicates superiority of radiation induced deletion and radiation hybrid mapping over mapping based on recombination.

Key words: Wheat, Fusarium head blight, Radiation hybrid mapping, Radiation induced deletion mapping, *Qfhs.ifa-5A*

ZUSAMMENFASUNG

Ährenfusariose ist eine bedeutende Pilzkrankheit die bei Weizen und anderen Getreidearten zu erheblichen Ertrags- und Qualitätseinbußen führen kann. Ein wichtiges Resistenz Quantitativer Merkmals Locus (QTL) in Weizen ist *Qfhs.ifa-5A*, welcher am Chromosom 5A zwischen den Markern *barc186* und *barc180* lokalisiert ist. Das QTL-Intervall hat eine Länge von 2,8 cM und erstreckt sich über das Centromer. Durch diese centromer-nahe Lage ist die Feinkartierung von *Qfhs.ifa-5A* erschwert, da die Rekombinationsrate nahe dem Centromer sehr gering ist. Kartierungsversuche mit Populationen aus bi-parentalen Kreuzungen, die auf Rekombination basieren, hatten daher wenig Erfolg das *Qfhs.ifa-5A* Intervall einzuschränken.

In dieser Arbeit wurde eine Deletionskartierung vorgenommen um die Auflösung im *Qfhs.ifa-5A* Bereich auf 5AS zu erhöhen. Es wurden durch Mutagenese mit Gammastrahlung zwei unterschiedliche Deletions-Populationen geschaffen. Eine Population wurde entwickelt durch Samen-Bestralung einer nah-isogenen Linie mit *Qfhs.ifa-5A* (NIL3) mit anschließender Selbstbestäubung zur M_2 oder M_3 Generation (Del-NIL3-Population). Für die zweite Deletions-Population wurde Pollen der Sorte Chinese Spring bestrahlt und damit die Chinese Spring-Deletionslinie ohne dem 5A Chromosome bestäubt (CS-RH-Population). Insgesamt wurden 1764 Del-NIL3 und 276 CS-RH-Linien mit 35 molekularen Markern genotypisiert. Die Ergebnisse beider Populationen positionierten neun Marker im telomer-nahen Bin, 5AS3-0.75-0.97, 13 Marker im Bin 5AS1-0.40-0.75 und 13 Maker im centromer-nahen Bin C-5AS1-0.40. Die CS-RH-Population zeigte eine höhere Anzahl von Deletionen, die Deletionen waren auch länger als in der Del-NIL3-Population. Die kleineren Deletionen im Del-NIL3-Panel führten aber zu einer besseren Auflösung.

Es wurde eine Konsensus-Karte aus 28 Del-NIL3 und 40 CS-RH Linien mit einer Länge von 324,8 cR erstellt. Mit einer Auflösung von 0,88 Mbp/cR hatte die Konsensus-Karte eine 253-fach höhere Auflösung als die genetische Karte für das Intervall *barc186-cfa2250*. Diese markante Verbesserung der Kartenauflösung im centromer-nahen Bereich zeigt die Überlegenheit des Strahlungsinduzierten Deletions-Kartierungsansatzes im Vergleich zu Kartierungen die auf Rekombination beruhen.

Schlüsselwörter: Weizen, Ährenfusariose, Deletions-Kartierung, induzierte Deletionen, Qfhs.ifa-5A

Table of Contents

Index of Tables

Illustration Index

LIST OF ABBREVIATIONS

BC	Backcross
cM	Centimorgan
cR	Centiray
CS	Chinese Spring
CS-DT5AL	Chinese Spring ditelosomic-5AL aneuploid line
CS-N5AT5B	Chinese Spring nullisomic-5A-tetrasomic-5B aneuploid line
CS-RH	Chinese Spring radiation hybrid
Del-NIL3	Radiation induced deletion on near isogenic lines
DGRH	D genome radiation hybrid
DH	Double haploid
DNA	Deoxyribonucleic acid
DSB	Double strand break
DT	Di-telosomic
EST	Expressed sequence tags
FHB	Fusarium head blight
GSS	Genome survey sequences
Gy	Gray
ISBP	Insertion site-based polymorphism
Kbp	Kilobase pair
krad	Kilo rad
LOD	Logarithm of odds
Mbp	Megabase pair
NGS	Next generation sequencing
NHEJ	Non-homologous end-joining
NIL-RIL	Near isogenic recombinant inbreed lines
NIL	Near isogenic lines
NT	Nullisomic-tetrasomic
PCR	Polymerase chain reaction
POPSEQ	Population sequencing
QTL	Quantitative trait loci
RH	Radiation hybrid
scs^{ae}	Species Cytoplasm specific gene
SNP	Single nucleotide polymorphism
SSR	Simple sequence repeats
TE based	Transposable element based
WGRH	Whole genome radiation hybrid

1 INTRODUCTION

1.1 Fusarium Head Blight

Fusarium Head Blight (FHB), also known as scab, is a severe fungal disease of wheat (*Triticum aestivum*) and other cereals, caused by *Fusarium spp*. FHB leads to drastic losses in yield quantity and quality, but the major risk represent the mycotoxins accumulated in the edible parts (Ban and Watanabe, 2001, Buerstmayr et al., 2002, Buerstmayr et al., 2003).

Schroeder and Christensen (1963) proposed a two components model of resistance, (i) Type I, against initial infection, and (ii) Type II, against spread of pathogen, which is later extended with additional three parameters (Mesterhazy et al., 1999): (iii) resistance to toxin accumulation, (iv) resistance to kernel infection, and (v) tolerance. Resistance to fungal spread plays a major role in the FHB resistance, as it explains up to 60% of the phenotypic variance for FHB resistance (Bai et al., 1999, Buerstmayr et al., 2002). Buerstmayr et al. (2002) reported a quantitative trait loci (QTL) on 5A chromosome, associated with Type I resistance. The identified resistance QTL *Qfhs.ifa-5A* was allocated in the 5A interval *gwm293-gwm156* (Buerstmayr et al., 2003) (Figure 1a) which is most likely positioned close to the centromere (Buerstmayr et al., 2009). An association of the pericentromeric interval of chromosome 5A to FHB resistance traits was repeatedly verified. Buerstmayr et al. (2009) summarized FHB QTL associated with type I resistance, derived from nine different resistance donors co-locating on 5AS (Figure 1b).

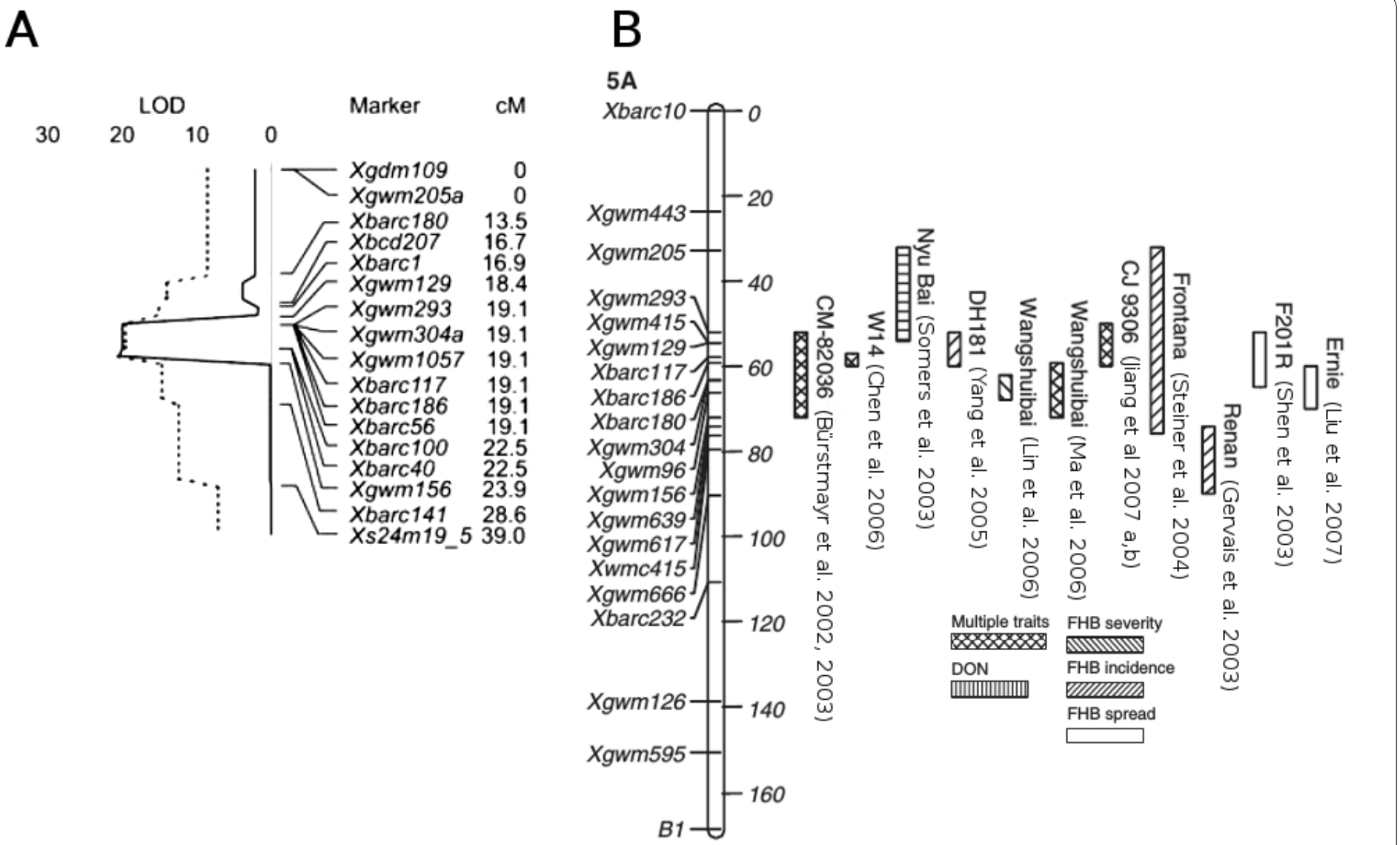

Figure 1 *Position of FHB resistance QTL on 5A wheat chromosome.* (**A**) *Interval analysis of the 5A QTL for the percentage of infected spikelets 26 days after inoculation. LOD values were calculated by composite interval mapping (solid line) and simple interval mapping (dotted line). The most likely position of the Qfhs.ifa-5A is in the Xgwm293-Xgwm156 interval (Buerstmayr et al., 2003).* (**B**) *FHB resistance QTL derived from nine different resistance donors co-locating on 5AS. QTLs are identified with the name of the cultivar contributing the resistant allele. Bars indicate QTL location (shorter bar means more precise location), and patterns of bars indicate the FHB-associated trait(s)-see legend (Buerstmayr et al., 2009).*

Qfhi.nau-5A (syn *Fhb5*) in the FHB resistant wheat germplasm Wangshuibai is a major QTL for type I resistance. Through multiple-year trials, this 5A QTL explained 16.6-27.0% phenotypic variation in the recombinant inbreed lines (RIL) population (Lin et al., 2006). Precise mapping of the *Fhb5* allocated the QTL to the pericentromeric interval of 5AS (Xue et al., 2011). The map assigned, through deletion bin mapping, the *Fhb5* to the pericentormeric C-5AS3-0.75 bin (Figure 2).

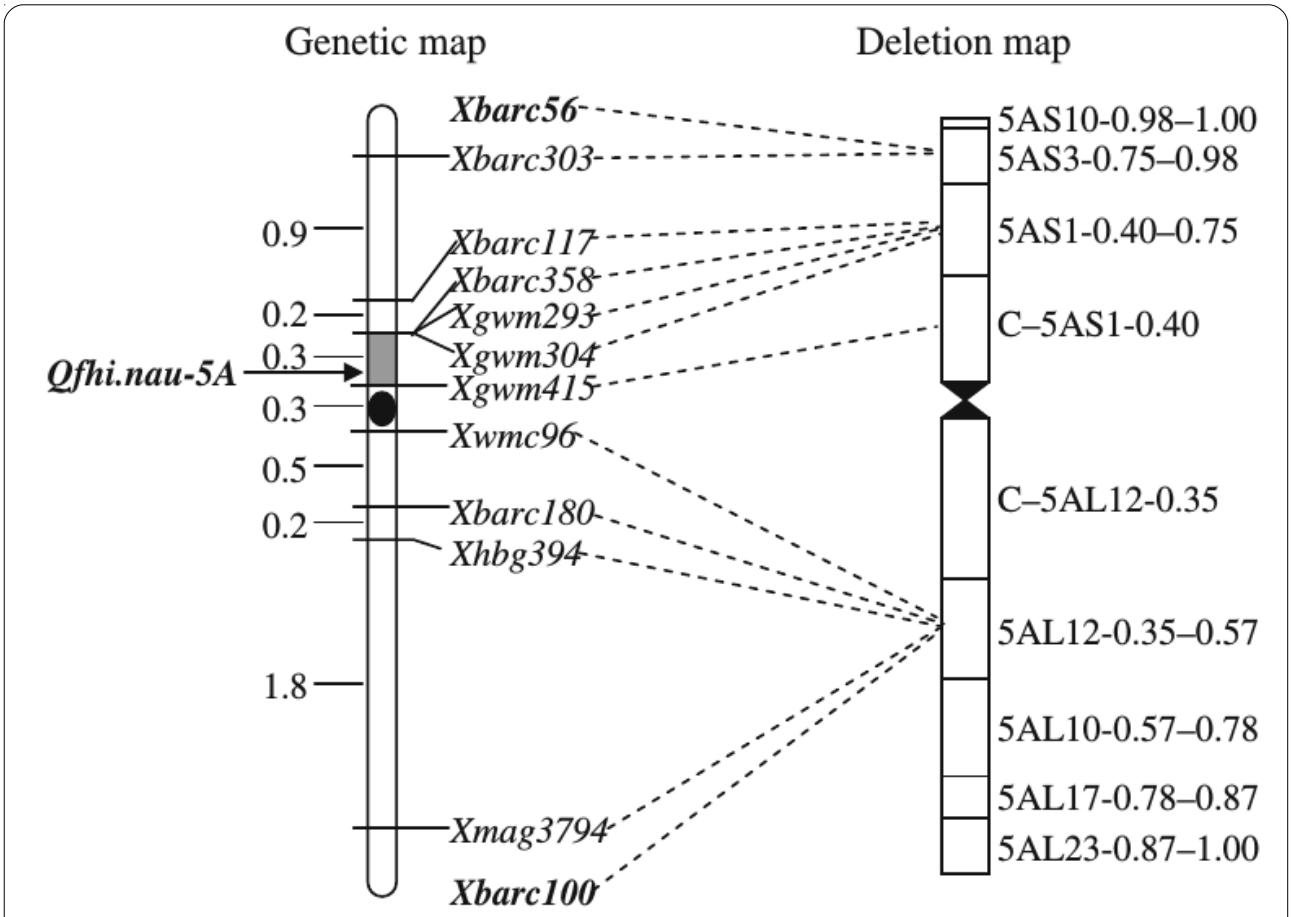

Figure 2 *Genetic map of the Qfhi.nau-5A region (left), with the markers assigned to the deletion bin of the 5A chromosome (right). Short arm is at the top, and the black oval indicates the centromere. Numbers on the left are genetic distances (cM). The bin assignments are shown on the right. Dashed lines position the markers into the bins (Xue et al., 2011).*

1.2 Mapping

Mapping is the process of determining the linear order of and relative distances between genes and/or molecular markers on a chromosome in the analysed material. There are two distinctive types of maps: genetic or linkage maps, based on recombination in segregating population, and physical maps which provide physical order and distances of the markers along the chromosomes.

1.2.1 Linkage (genetic) Mapping

Genetic mapping has been extensively used ever since the first map was published by Sturtevant (1913). A linkage or genetic map relies on the number of crossover events and recombination frequencies between markers. Generating such map is based on the independent assortment of chromosomal segments during meiosis. If genes, markers or chromosomal segments do not assort independently, they are considered to be linked. Recombination rate and the probability that a recombination occurs between two loci depends on their physical distance. The shorter the distance between two loci, the higher the probability that they will stay together during meiosis. With increasing distance between two points on the chromosome, increases the probability for a recombination to occur. In this way genetic linkage represents the physical distance. However, recombination is not uniform across the genome, as it is affected by chromosome structure and varies across the length of chromosomes (Kalavacharla et al., 2009).

Kumar et al. (2015) point out the three major limitations for recombination mapping approach: (i) The necessity of polymorphic markers. Selection pressure excludes non-favorable allelic polymorphism in the gene space, leading to high intraspecies monomorphism. (ii) Variation in recombination rates along the length of chromosomes (Gill et al., 1993, Lukaszewski and Curtis, 1993, Akhunov et al., 2003, Saintenac et al., 2009). In the centromeric regions the recombination frequency is close to zero, while with increasing distance from the centromere, the recombination increases by approximately the square of the relative distance (Künzel et al., 2000, Akhunov et al., 2003). More than 85-fold difference was observed for genetic to physical distance ratio (cM/Mb) between the bin closest to the centromere (C-3BS1-0.33) and the bin positioned at the telomere (3BS8-0.78-0.87) on wheat chromosome 3B (Saintenac et al., 2009). Paux et al., (2008) reported

that 2.2 % of the genetic map length in the centromeric regions actually represents 42 % of the physical map length of chromosome 3B. Consequently, there is discrepancy between genetic and actual physical distances. Low recombination regions aggravate developing high resolution genetic maps and cloning a gene of interest positioned in the same area. (iii) Large populations are inevitable in order to achieve higher resolution.

Sakai et al. (2009) compared physical and genetic maps of the 3H barley chromosome. Firstly they constructed the cytological map of the 3H, after which they used the same expressed sequence tags (EST) markers to assemble a 3H genetic map. For the low recombination frequency around the centromere, genetic mapping was not able to precisely locate the centromere, while physical mapping identified the position of the centreomere. Nevertheless, genetic map in this case demonstrated superiority over the physical map in effectively separating clusters of EST markers that were congregated by the physical mapping.

1.2.1.1 Genetic Mapping of Qfhs.ifa-5A Utilizing Near Isogenic RIL Population (NIL-RIL)

Previous study conducted at IFA analysed 3650 BC_5F_2 plants (unpublished data), derived from crossing NIL1 (near isogenic line) to NIL2 (Schweiger et al., 2013). NIL-RIL population (BC_5F_2) has the genetic background of Remus, with fixed *Fhb1* (Buerstmayr et al., 2002), but segregating for *Qfhs.ifa-5A*. To create NILs, DH lines (CM-82036 x Remus) containing *Fhb1* and *Qfhs.ifa-5A* were backcrossed with Remus five times. NIL1 possesses resistance alleles for *Fhb1* and *Qfhs.ifa-5A*, while NIL2 bears resistance only for *Fhb1*. Of 3650 BC_5F_2 plants only those with recombination in the *Qfhs.ifa-5A* support interval of interest were selected for further fine mapping with 16 available polymorphic markers. Seventy-two recombinant NILs were subjected to field tests to validate their FHB resistance, in two consecutive years (2014 and 2015). QTL interval was positioned between *barc186* and *barc180* flanking markers, spreading across the centromere and covering the distance of 2.8 cM (Figure 3). Sixteen markers were allocated to 9 loci, and analysed lines formed 16 haplotypes.

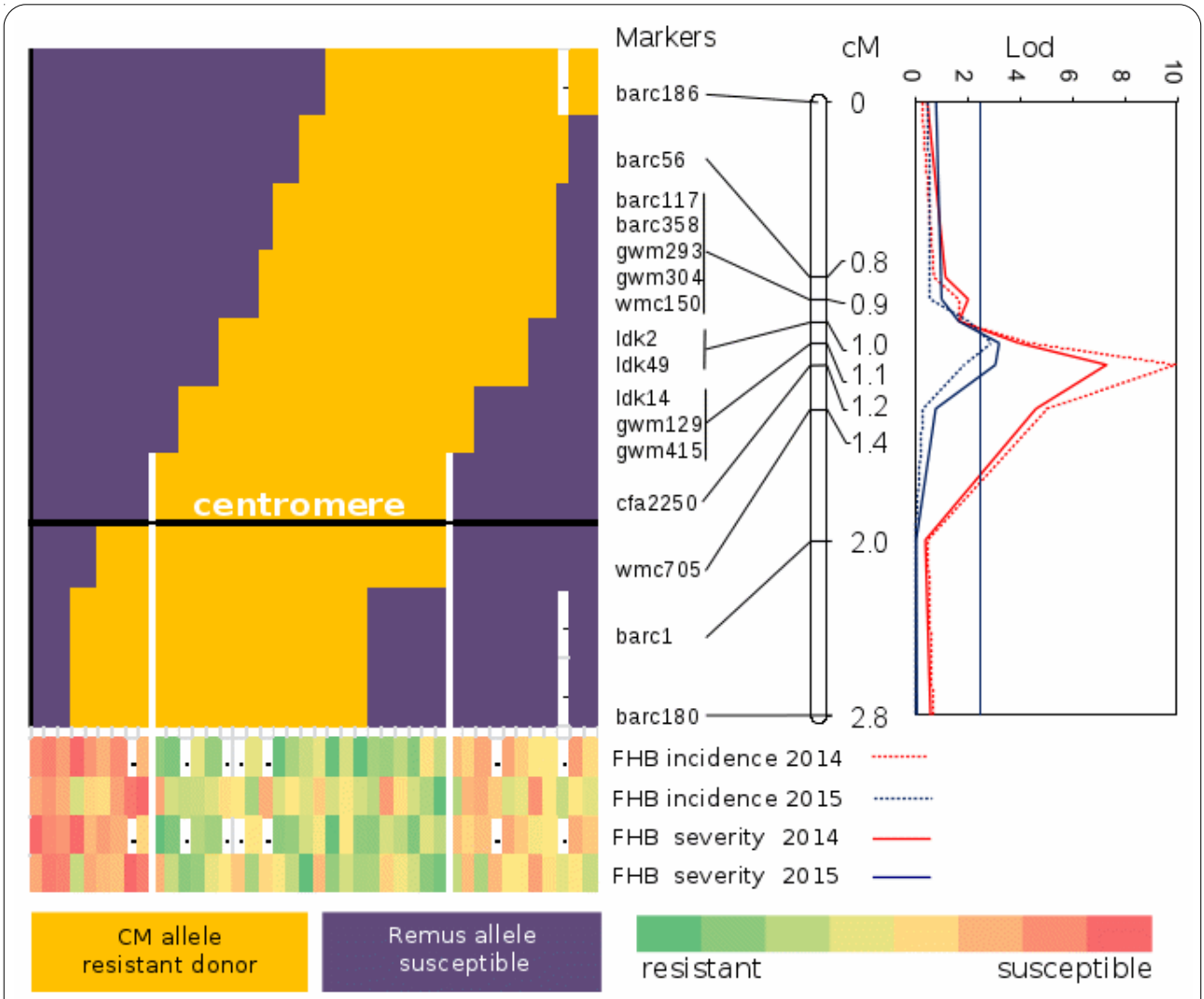

Figure 3 *Graphical illustration of the recombinant genotypes in the Qfhs.ifa-5A interval. Purple colour represents Remus (susceptible) and yellow CM (resistant) allele. Black horizontal line indicates centromere. Below are phenotypical results for FHB incidence (dashed line) and severity (solid line) in two consecutive years, 2014 (red lines) and 2015 (blue lines). Phenotypic scoring is presented on a colour scale from green (resistant) to red (susceptible). White vertical lines highlight a change in response at marker cfa2250. It is evident that lines carrying CM allele are resistant. On the right is genetic map consisting of 16 polymorphic markers which were mapped to nine loci. The whole map covers 2.8 cM.*

1.2.2 Deletion Bin Mapping

Physical positions of markers on any given chromosome or chromosomal segments can be assigned by using aneuploid lines derived from the hexaploid Chinese Spring (CS), such as nullisomic-tetrasomic (NT), di-telosomic (DT), and deletion bin lines. Sears (1954) developed wheat lines missing entire chromosome or chromosome arms. Chromosomal structural changes were induced by gametocidal chromosome of *Aegilops cylindrica* (Endo, 1988), creating deletions of the distal chromosome segment from the initial breakpoint (Endo, 1990). Totally, 430 deletion stock lines for 21 wheat chromosomes have been created (Endo and Gill, 1996), and are intensively used in physical and cytological chromosome mapping (Barabaschi et al., 2015; Gadaleta et al., 2012; Qi et al., 2004; Werner et al., 1992; Xue et al., 2011). For 5A chromosome, there are 11 short arm deletions and 23 in the long arm (Endo and Gill, 1996) (Figure 4). Although deletion mapping can correct for some mistakes in genetic mapping, because it allows assigning marker to a chromosomal region, the linear order of markers within the bin interval is still unknown.

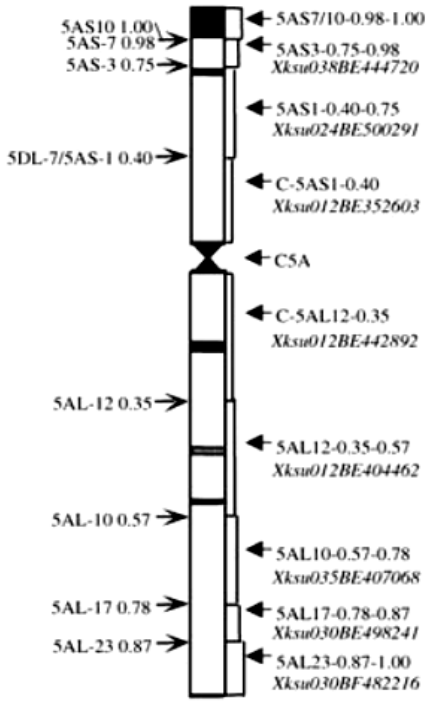

Figure 4 *The partitioning of the 5A wheat (T. aestivum, cv Chinese Spring) chromosome into bins based on deletion breakpoints. On the left are indicated names of the deletion lines and the fraction length values, on the right is the bin assignment (Qi et al., 2003).*

1.2.3 Radiation Hybrid Mapping

Radiation hybrid (RH) mapping is an alternative method to genetic linkage mapping. It uses radiation induced chromosomal breaks and the frequency of co-retention between markers to map them on a chromosome. It was first described by Goss and Harris (1975), who induced chromosomal breaks by X-rays to create a map of the human X chromosome. High irradiation dosage creates double strand breaks (DSBs) across the genome. The two main repair mechanisms, homology-directed repair and non-homologous end-joining (NHEJ), recognize and repair the breaks (Britt, 1999, Bernstein and Rothstein, 2009). Both mechanisms are highly conserved in eukaryotes, although NHEJ dominates in higher eukaryotes. NHEJ is error prone and it is the source of different genomic rearrangements, such as interstitial deletions, translocations, insertions, and inversions (Puchta, 2005). Ataxia Telangiectasia Mutated signalling pathway recognizes the broken DNA ends, triggering the *Ku* protein complex, which protects the DSBs from degradation by hooking at the break sites. DNA Phosphokinases dock to the complex and create protein bridges that connect the broken ends together and re-join them by a DNA ligase. By re-joining broken ends, the adjacent nucleotides are lost creating smaller or larger deletions (Britt, 1999, Bleuyard et al., 2006, Bernstein and Rothstein, 2009).

Radiation induces breakages randomly and homogeneously across the chromosome (Riera-Lizarazu et al., 2000, Gao et al., 2006, Riera-Lizarazu et al., 2010). Similarly as in the genetic maps, the higher the physical distance between two loci is, the more likely will the applied radiation dosage break them apart. The distance between loci and their relative arrangement is determined by calculating the frequency of co-retention between markers (Kumar et al., 2014). The radiation hybrid map unit of distance is centi-Rays (cR). Centi-Rays are not a constant unit, but the value depends on the specified dose of radiation used to break the DNA into fragments. Value of one centi-Ray refers to a chromosomal interval within which there is 1% probability to induce break at a given dose of radiation (Womack et al., 1997).

1.2.3.1 Advantages of RH Mapping

1.2.3.1.1 Uniform Mapping Resolution Across the Chromosome

Genetic mapping is based on recombination events, which are unevenly distributed throughout the chromosomes (Gill et al., 1993, Lukaszewski and Curtis, 1993). The recombination rate decreases with proximity of centromere (Akhunov et al., 2003), thus impeding the high density mapping of pericentromeric regions using genetic mapping populations. RH mapping, as a recombination independent approach, overcomes the difficulties in genetic mapping due to randomly induced deletions, providing homogeneous resolution across the length of a chromosome. In a study in maize, results demonstrated that radiation induced deletions along the chromosome 9 were homogeneous, without preferential breakage spots on a specific chromosomal region (Riera-Lizarazu et al., 2000). Similar uniform marker losses were reported in wheat (Riera-Lizarazu et al., 2010), and in cotton (Gao et al., 2006). These finding were additionally supported by comparing genetic and RH map of wheat chromosome 3B (Kumar et al. 2012a). RH map provided 10.5 fold higher resolution and 6 fold more uniformity. Additionally, Kumar et al., (2012a) observed a strong correlation between the DNA breakage and the frequency of meiotic recombination. These results suggest that the state of chromatin might affect formation of chromosomal deletions in a similar way it has on recombination.

1.2.3.1.2 Higher Mapping Resolution

The resolution of a RH map depends on the number of breaks along the chromosome, which can be influenced by altering the radiation dose. Low, medium, and high resolution panels can be created by modifying radiation dosage. Increasing γ-radiation dose leads to increase in marker loss and chromosome rearrangements. Therefore, it is possible to produce RH panels with higher resolution without increasing the population size. For example, in cotton, 80 Gy induced more breaks and more deletions than 50 Gy (Gao et al., 2004, Gao et al., 2006). However, plants have limited tolerance for the radiation dosage, because higher dosage leads to highly fragmented chromosomes which rarely survive the cell division. Increased radiation dosage causes lower germination rate, plant survival, and vigor (Riera-Lizarazu et al., 2000, Gao et al., 2006), as seen from the results presented by Hossain et al. (2004a) where dosage over 40 krad resulted in dramatic reduction in

survival and plant vigor. Thus, the optimal dosage which induces maximal chromosomal breaks with maximum plant survival and seed set must be determined for each species.

1.2.3.1.3 Mapping of Monomorphic Markers

RH mapping is based on presence (retention) or absence (deletion) of marker loci, which allows the use of monomorphic markers.

1.2.3.2 Genetic vs RH Maps

Kumar et al., (2012a) compared the results obtained from the RH map of the 3B chromosome with the genetic map published by Saintenac et al. (2009). 3B-RH map was constructed on 92 lines and it showed a 10.5 fold higher overall resolution than the genetic map (using ~400 doubled haploid lines). RH map obtained a 136-fold increased map resolution in the centromeric region, and six times more uniform overall resolution than the genetic map. Results from RH map for chromosome 2D were compared to published genetic map. The 2D-RH map provided 5.2-fold higher resolution. The genotyping data for the 25 markers on 92 $DGRH_1$ lines formed a map spanning 453 cR, with 15 loci. Comparison of the 2D-RH map with a genetic map showed a cM/cR ratio of 1/5.2 (Kumar et al., 2012b).

Tiwari et al., (2016) developed a whole-genome radiation hybrid (WGRH) map and compared results with existing genetic maps. The efficiency of the calculated map was compared to the eight genetic maps developed from double-haploid (DH) wheat mapping populations (Wang et al., 2014). The RH panel mapped more markers in each genome (A, B, D) than any of the eight DH populations, with the greatest difference observed in the D genome. The WGRH map allowed anchoring three- to six-fold more markers for the D genome. Additionally, RH panel showed three- to eight-fold increase in resolved bins across the entire wheat genome. Marker order and the integrity of the RH map were confirmed by comparing mapping bins to Population sequencing (POPSEQ) resource (Chapman et al., 2015), where genetic map was derived from 90 DH lines (synthetic W7984 x Opata (SynOpDH) population (Sorrells et al., 2011)). The average mapping resolution provided by the RH map was five-fold greater than the average resolution in the POPSEQ. Furthermore, order of markers on the RH map of the chromosome 7D was compared to the order of markers in the SNP-based consensus genetic map (Wang et al., 2014) to validate marker ordering. Chromosome 7D was chosen due to the best marker

coverage in the both WGRH and SNP-based concensus genetic map. The genetic SNP map had better resolution in the telomeric regions of the chromosome, while the WGRH map provided better resolution in the centromeric regions. WGRH map was compared to the reference sequence of chromosome 3B (Choulet et al., 2014) to verify the ordering potential and estimate the mapping resolution of the WGRH map for that chromosome. WGRH panel mapped 3.4-fold more markers, and provided an average mapping resolution of 0.53 Mb/cR$_{1500}$.

Radiation hybrid map of barley chromosome 3H had a resolution ~9-fold higher than a genetic map, reaching the maximum of more than 262.40-fold resolution in the pericentromeric regions (Mazaheri et al., 2015).

1.2.3.3 RH Panels in Plants

In humans and animals, mapping strategy relies on somatic hybridization, where donor cells are irradiated to induce breaks and fused to non-irradiated recipient cells of a distinct species, followed by *in vitro* cell culture. In plants, both *in vitro* (de Bona et al., 2009; Wardrop et al., 2004, 2002; Zhou et al., 2006) and *in vivo* (Gao et al., 2006, 2004; Hossain et al., 2004b; Kalavacharla, 2006; Kumar et al., 2012a, 2012b; Paux et al., 2008; Riera-Lizarazu et al., 2010, 2000) techniques can be used to develop RH panels. Somatic cell hybridization, despite the extensive use for animal gene mapping, in plants has technical limitations, such as: (i) finding an appropriate recipient cell line to rescue irradiated chromosomes; (ii) stability of tissue culture, (iii) limited amount of DNA, and (iv) inability to produce viable plants for functional analysis (Wardrop et al., 2002).

In plants, irradiating seeds or pollen is often used to establish RH mapping population. Through meiosis, the irradiated material with highly fragmented chromosomes may not survive the following cell division. However, plants that survive constitute a stable, viable, and fertile genetic source (Gao et al., 2006, 2004; Kumar et al., 2012b; Riera-Lizarazu et al., 2010, 2000), which can be used to identify genomic regions associated with a phenotype of interest (Hossain et al., 2004b, Bassi et al., 2013, Michalak de Jimenez et al., 2013). On the other hand, gamete (pollen) irradiation causes chromosome breaks after the final microgametophyte mitotic division, thus circumventing meiotic sieving. Treated pollen is used to fertilize non-irradiated material and due to the presence of at least half non-damaged material the chances for survival of the M_1 plants carrying deletions increases (Tiwari et al., 2012).

1.2.3.4 Marker Retention Frequencies in RH Panels

Marker retention frequency is the percentage of a marker retained across the population. Studies suggested that the optimal retention/loss frequency for the mapping purposes should be 50% (Jones, 1996). The necessary retention frequency is achievable through protoplast cell fusion (Wardrop et al., 2004). It has been reported that *in vivo* RH panels less than 0.5% of the lines show retention frequencies between 40 and 60% (Bassi et al., 2013; Kumar et al., 2012a; Michalak de Jimenez et al., 2013). Overall, RH studies in plants report marker retention between 75 and 97 % (Gao et al., 2006; Hossain et al., 2004b; Kalavacharla, 2006; Tiwari et al., 2012). Studies on wheat D genome showed an average retention of 74 % in the RH panel created from irradiated seeds (Kalavacharla, 2006; Michalak de Jimenez et al., 2013), while 86.2 % under 15-Gy dosage of pollen irradiation (Tiwari et al., 2012). An average marker retention in a WGRH mapping of hexaploid wheat was 79%, 77%, and 80% for the A, B, and D genome, respectively, by pollen irradiation technique (Tiwari et al., 2016).

1.2.4 Applications and Prospects for RH

1.2.4.1.1 RH for Mapping and Cloning Genes

Genomic location is important for any comparative mapping study and/or positional cloning. Aneuploid lines and cytogenetic stocks are used to localize genes to a region on a chromosome. In wheat, Endo and Gill (1996) developed a set of 436 terminal chromosome deletions utilizing gametocidal genes to induce chromosomal breaks. These breaks divided the whole wheat genome into large segments (on average 40 Mb). Deletions stocks together with nullisomic-tetrasomic (NT) lines (Sears, 1966, 1954), and ditelosomic (DT) lines were used to map over 7.000 ESTs in wheat (Conley et al., 2004; K. G. Hossain et al., 2004b; Linkiewicz et al., 2004; Miftahudin et al., 2004; Munkvold et al., 2004; Peng et al., 2004; Qi et al., 2004; Randhawa et al., 2004). Deletion mapping has several drawbacks: (i) only certain *Aegilops* species provide necessary gametocidal genes, and their transfer into lines of interest can be difficult; (ii) breaks induced this way are non-random and terminal (Sakai et al., 2009); (iii) due to the limited number of deletion lines, in some cases this mapping approach yields lower resolution than genetic mapping; and (iv) although it is possible to allocate genes and sequences to chromosomes or a large

segment of a chromosomes, it is impossible to order the sequences within the particular chromosomal segment.

Radiation hybrids can be used for mapping similarly as cytogenetic stocks, but at a much higher resolution. RH induces random breaks that can cause terminal or interstitial deletions (Hossain et al., 2004b; Kalavacharla, 2006; Paux et al., 2008; Sakai et al., 2009) and the number of breaks can be manipulated by the applied dosage.

Positional cloning utilizing a genetic mapping is tedious and not always successful procedure, due to the limitations posed by genetic mapping, such as need of a large population, availability of polymorphic markers, and the poor conversion of genetic to physical distances (Salvi and Tuberosa, 2005). RH easily overcomes these limitations. Fine mapping or cloning a QTL is usually conducted on NILs, which segregate only for the interesting interval. Developing NILs is time consuming, as it takes four to six generations. On the other side, RH population can easily be created in only one generation. Furthermore, positional cloning requires a large number of polymorphic markers. To develop a high resolution map, numerous markers must be tested for polymorphism between the parents. Testing for polymorphism is a tedious task in positional cloning, especially in non-sequenced organisms. Positional cloning utilizing RH panel is advantageous as non-polymorphic markers can be used. Therefore, the RH method is suitable for high-throughput genotyping. Moreover, RH method can be used for mapping, cloning, and characterization of monomorphic genes lacking any natural variation, such as genes controlling life-dependent functions.

Finally, due to the different recombination frequencies across the length of the chromosome it is not possible to precisely determine the physical position in low-recombinogenic regions employing genetic mapping. RH mapping distances are based on breakages that occur randomly in the genome, and thus provide better estimation of actual physical distances (Kumar et al., 2012a). RH mapping effectively facilitates mapping and positional cloning by shortening the amount of time needed for high resolution mapping.

1.2.4.1.2 RH Mapping and Forward/Reverse Genetics

Forward genetic approach investigates the underlying genetic mechanism for a particular phenotype. Reverse genetics seeks to identify the phenotype of a particular genetic sequences.

RH in the reverse genetic studies has been mainly limited to insects and animals. X-ray induced mutation in *Drosophila melanogaster* in chaoptic (*chp*) gene sequence reduced protein level enabling a functional phenotypic analysis (Van Vactor et al., 1988). Embryonic stem cells of mice were irradiated to observe changes in phenotype due to loss of genes at the *D17Aus9* locus (You et al., 1997). Phenotypic changes resulted in individuals runt in size and carrying shortened or kinked tail.

The forward genetic approach using induced mutations has been applied in *Arabidopsis*, rice, tomato, and wheat. M_2 *Arabidopsis* population created by fast neutron radiation contained mutants such as in gibberillic acid sensitive, hypocotyl morphology, narrow leaves, double flower, and trichome mutants (Koornneef et al., 1982; Koornneef and Veen, 1980). Further work led to the cloning of genes involved in testa color such as chalcone flavanone isomerase and dihydroflavonol 4-reductase (Shirley et al., 1992), and positioning the genes related to plant height and flowering onto chromosomes (Koornneef et al., 1991). So far, deletion rates in animal RH panels have been higher than those observed in plants. Low deletion rates make it possible to develop *in vivo* viable plant populations. Plant RHs, when compared to animal, are easy to develop, reproducible and ethically acceptable. RH populations are excellent in forward/reverse genetic studies to identify effects of gene modification to related phenotype and to associate altered phenotype with its genotype.

1.2.4.1.3 RH Mapping and Comparative Genomics

Comparative genomic studies between species elucidate chromosome evolution, and provide knowledge about genome structure. In animals, RH maps and sequences of model species have been used in synteny studies. Chromosome evolution in mammals has been analysed utilizing whole genome comparative analysis, based on RH maps. To face the fundamental questions about mammalian chromosome evolution, the information from the RH mapping of cat, cattle, dog, pig, and horse was compared to the whole genome sequences of human, mouse, and rat (Murphy et al., 2005). The study constructed an evolutionary scenario representing the rearrangements between all the genomes and their ancestors.

The whole genome comparative analysis provides valuable knowledge about the physical clustering of gene families across species, as well as identifying structural linkage associations conserved for millions of years across thousands of species (O'Brien et al., 1999).

There are only few comparative genome analysis in grasses. Currently only a few species are fully sequenced (Vogel et al., 2010), and for many other species only low resolution genetic and the chromosomal bin maps are available (Salse et al., 2008, Luo et al., 2009). This strongly limits our understanding of evolutionary mechanisms. Comparison of sequences of a species of interest with a model plant allows the identification of conserved syntenic intervals, and it assists in detecting important genes and clarifying the evolution of genomes (Kumar et al., 2014).

Syntenic analysis encounters two problems: low resolution in genetic maps and need for polymorphism. Low resolution allows detection of conserved regions at the macroscopic level (macro-colinearity), and it hampers separating markers making it impossible to determine whether these genes maintained their order or if rearrangement occurred through time. Further difficulties arise from selection pressure that excludes most non-beneficial allelic polymorphism in the gene space. For example, in hexaploid wheat 9.9% polymorphism was observed for EST-derived simple sequence repeats (SSRs), while 35.5% polymorphism was observed in the genomic SSRs (Xue et al., 2008).

Mapping monomorphic markers by RH significantly improves mapping resolution (de Pontbriand et al., 2002; Gautier and Eggen, 2004), which is beneficial for syntenic studies at microscopic levels (micro-colinearity). A study in wheat allowed to determine the ancestral origin of the centromere of chromosome 1D (Michalak de Jimenez et al., 2013), supporting a neocentromerization event as result of fusion two paleochromosomes.

High resolution RH maps can improve comparative genomics analysis and evolutionary studies, as they provide similar information as genome sequence assembly, but at a lower cost (Hitte et al., 2005).

1.2.4.1.4 RH Mapping and Survey Sequencing

Newly developed next-generation sequencing (NGS) platforms provide extensive sequence information (Gupta, 2008; Metzker, 2010). NGS led to sequencing a whole genome for some plant species (Feuillet et al., 2011). Genome Survey Sequences (GSS), nucleotide sequences with genomic origin, are used in mapping studies, as well in comparative analysis. GSS combined with RH mapping is a valuable tool for acquiring genomic information at a lower cost, and has been proven in creating a high-quality comparative map (Hitte et al., 2005).

1.2.4.2 RH Mapping in Wheat

To create RH lines in wheat the following approaches were used: aneuploid stocks (Paux et al., 2008, Yamano et al., 2010, Kumar et al., 2012a, Bassi et al., 2013), asymetric hybridization (Zhou et al., 2012), and panels hemizygous for the D genome by crossing irradiated hexaploid wheat to non-irradiated tetraploid wheat (Hossain et al., 2004b, Kalavacharla, 2006, Riera-Lizarazu et al., 2010, Kumar et al., 2012b, Tiwari et al., 2012, Michalak de Jimenez et al., 2013, Kumar et al., 2015). RH in wheat has been successfully used for mapping a specific gene or parts of a chromosome (Hossain et al., 2004b, Yamano et al., 2010, Bassi et al., 2013), single chromosome (Kalavacharla, 2006, Paux et al., 2008, Michalak de Jimenez et al., 2013, Kumar et al., 2012a, Zhou et al., 2012), D genome (Kumar et al., 2012b, Tiwari et al., 2012, Kumar et al., 2015) or the whole genome (Tiwari et al., 2016).

Hossain et al., (2004b) first reported using RH mapping to localize a specific gene in wheat. Species Cytoplasm-Specific (*scs*^{ae}) gene was mapped on the long arm of chromosome 1D utilizing RH population derived from gamma irradiated hemizygous line. In the study was noticed that applied radiation dosage above 40 krad results in drastic decrease in survival and plant vigor. The average marker retention frequencies in this study ranged from 87% to 100%. First high-resolution RH map of wheat chromosome 1D had an estimated resolution of ~199 kb/break (Kalavacharla, 2006). An RH panel of 87 lines was used to map 378 markers. Average marker retention frequency was 74%. Total map distance for a comprehensive map covered 11773 cR_{35000}. Michalak de Jimenez et al. (2013) used RH methodology to refine the location of the *scs*^{ae} gene on 1D chromosome. Genotyping 188 individuals with 57 markers created RH map covering 205.2 cR. Previously the *scs*^{ae} was located on a region of ~8.3 Mbp, but through forward genetics in this study it was pinpointed to a 1.1 Mbp segment. Riera-Lizarazu et al. (2010) presented a crossing scheme to produce radiation hybrids for the D genome (DGRH). Seeds of hexaploid wheat (AABBDD) are irradiated, planted and the surviving plants ($DGRH_0$ generation) are crossed to tetraploid wheat (AABB). Generated panel of quasi-pentaploids ($DGRH_1$ generation) allows detection of all lesions on D genome chromosomes. Marker retention frequencies were homogenous along the chromosome, proving the random induced breakages. The average marker retention frequencies ranged from 94.4 to 98.6%. This method for production RH panels for the D genome has later been utilized by Kumar et al. (2012b) and Tiwari et al. (2012). Kumar et al. (2012b) characterized a panel of 1510 RH_1 plants. RH_1 originated from irradiated seed of a synthetic hexaploid (AABBDD) wheat

with the D genome of *Aegilops tauschii*. The average marker loss (2.1%) was homogenous, but increase in the marker loss, as well as decrease in plant survival, was observed with an increase in radiations doses.

DGRH panel constructed from irradiated pollen was genotyped for deletions with 737 markers. Chinese Spring spikes were irradiated during flowering, and irradiated pollen was used for pollination. Embryo and endosperm were dissected from each F_1 seeds. Tiwari et al., (2012) created two subpanels from dissected embryos and endosperms. Endosperms tolerate more paternal radiation-induced chromosome aberrations than embryos due to genetic buffering by triploid endosperm.

RH mapping supported physical mapping of chromosome 3B (Paux et al., 2008). Yamano et al. (2010) created RH mapping population to localize gametocidal inhibitor gene (*Igc1)* gene in the pericentromeric region of the chromosome 3B. In total, 122 chromosome deletion lines derived from crossing irradiated 'Norin 26' pollen to 'Chinese Spring' 3B-3C substitution line were characterised with 102 markers. The average marker retention frequency in total 199 F_1 progeny was 95.75%. Kumar et al. (2012a) generated a high density RH map with 541 marker loci anchored to chromosome 3B covering a total distance of 1871,9 cR. This study showed that: (i) DNA break/repair mechanism shows correlation to the frequency of crossing-over, (ii) deletions in centromeric region are fewer but larger in size.

Zhou et al. (2012) assembled an RH map for the 5A chromosome based on genotyping results of 68 SSR markers. Two panels were developed by asymmetric somatic hybridization between wheat and *Bupleurum scorzonerifolium*. Comprehensive map covered 2103 cR, with estimated resolution ~501.6 kb/break.

A WGRH map of hexaploid wheat was published by (Tiwari et al., 2016). The whole map length was 6866 cR_{1500}, and it was constructed based on data obtained from 26299 SNP from 115 lines. The average mapping resolution was ~248Kb/cR_{1500}.

1.3 Aim of the Master Thesis and Research Questions

The general objective of this study was to provide a high resolution map for the pericentromeric region of the short arm of the 5A wheat chromosome and to produce viable seeds for testing in field experiments.

In total, 1764 mutants of an experimental line harboring *Qfhs.ifa-5A* were preliminary screened for deletions with 14 markers, and further genotyped with 35 markers. These deletions lines were created by irradiating seeds and propagating plants to M_2 and M_3 generation to increase the homozygosity. Additionally, 276 lines, originating from the cross between irradiated pollen of Chinese Spring cultivar and the aneuploid Chinese Spring line lacking the 5A chromosome (nulli-5A-tetra-5B, CS-N5AT5B), were characterized with all 35 markers. Radiation induced deletion map was compared with the genetic map obtained from genotyping the NIL-RIL population.

Characterisation of the Del-NIL3 and CS-RH panel addressed the following questions:

- Can radiation induced deletion mapping provide higher resolution for the pericentromeric region?
- Is there a difference between pollen irradiation and seed irradiation techniques in mapping resolution, and marker retention frequencies?

2 MATERIALS AND METHODS

2.1 Plant Material

2.1.1 Deletion Population of Near Isogenic Line (Del-NIL3)

CM-82036 (full name CM-82036-1TP-10Y-OST-10Y-OM-OFC) was created from Sumai#3 and Thornbird-S parental lines, as a results of a breeding program between CIMMYT Mexico and South-America. It expresses a high level of resistance against FHB, with the resistance derived from Sumai#3, as well as good agronomic adaptation. The Bavarian State Institute for Agronomy in Freising (Germany) produced a spring wheat cultivar Remus (Sappo/Mex//Famos), which exhibits good agronomic traits and adaptation for cultivation in central Europe, but it is susceptible to Fusarium (Buerstmayr et al., 2002). A DH population was generated from crossing the highly resistant CM-82036 with the susceptible Remus cultivar (Buerstmayr et al., 2002). Based on genotypic and phenotypic results, a DH line was selected and five times backcrossed to Remus cultivar to produce near isogenic lines. In each backcross step, NILs were screened for presence of *Fhb1* and presence of *Qfhs.ifa-5A* using flanking markers. Finally, BC_5 was self-pollinated and F_2 plants were screened for the presence of homozygous QTL. NIL3 carries the *Qfhs.ifa-5A* resistance allele, whose presence was verified by flanking SSR markers *barc186* on the short arm of chromosome 5A, and *barc1* on the long arm of 5A (Schweiger et al., 2013). NIL3 seeds were irradiated with 250 Gy γ-rays at the Department of Plant Science, North Dakota State University, Fargo USA (Shahrayr Kian laboratory). From each seed, two plants were further propagated to the M_3 generation. Moreover, NIL3 seeds were irradiated with 240, 270, 300, and 300 Gy at the IAEA (International Atomic Energy Agency) laboratories in Seibersdorf, Austria, and were selfed to M_2 generation. Eight hundred M_3 lines and 964 M_2 plants (in further text referred to as Del-NIL3 or seed irradiated panel) were used for genotyping and fine mapping.

2.1.2 Chinese Spring Radiation Hybrid (CS-RH)

Chinese Spring cultivar is widely used for cytogenetic research in wheat, due to high number of available aneuploid lines. Chinese spring pollen was harvested during flowering and irradiated with 100 Gy. The irradiated pollen (RH_0) was used to pollinate nulli-5A-tetra-5B (CS-N5AT5B) (Sears, 1966). CS-N5AT5B completely lacks the 5A chromosome, but instead carries four 5B chromosomes, thus created RH_1 is hemizygous for the 5A. RH lines derived from the Chinese Spring were kindly provided by Luigi Cattivelli (CRA, Fiorenzuola d'Arda, Italy). A panel of 276 lines (in further text referred to as CS-RH or pollen irradiated panel) was subjected for further genotyping.

2.2 Experimental Methods

2.2.1 Genotyping the Deletion Lines

2.2.1.1 DNA Extraction and Quantitation

DNA was extracted from young leaves of 1764 Del-NIL3 and 276 CS-RH individual seedlings by a customised Saghai-Maroof et al. (1984) protocol. Plant material was dried at 36°C and ground to powder with a mechanical mill (Retsch, MM301) in 1.2 ml eight tube-strips containing five to seven glass beads per tube. Plant powder was dispersed in 700 µl extraction buffer (100 mM Tris pH 7.5, 700 mM NaCl, 50 mM Ethylenediaminetetraacetic acid, 1% (w/v) hexadecyltrimethylammonium bromide, 140 mM 2-mercaptoethanol) followed by incubation at 65°C for 60 to 90 minutes with gentle swirling. Afterwards, 350 µl chloroform:isoamylalchohol (24:1) (vol/vol) was added to each tube and mixed by gentle inversion for ten minutes. Stripes were centrifuged at 4000 rcf for ten minutes. Unless stated otherwise, all centrifugation steps were done at room temperature in Sigma Laboratory Centrifuges, 4 K 15. Post centrifugation, 300 µl supernatant was transferred into a new tube, to which 300 µl of isopropyl alcohol was added. Prior next centrifugation at 1000 rcf for eight minutes, tubes were slowly inverted allowing DNA to precipitate. Centrifugation formed pellets adhering at the bottom of the tubes, enabling supernatant to be discarded without losing the DNA. Obtained pellets were purified with two washing steps (‘*Wash 1’* 200 mM sodium acetate, 76% Ethanol; and *‘Wash 2’* 10 mM ammonium acetate, 76% Ethanol, respectively), with centrifuging at 1000 rcf for eight minutes after each washing step. Pellets were air dried overnight and dissolved in 100 µl 0.5x TE-8 buffer.

Isolated DNA was quantified by absorption at 230, 260, and 280 nm (Gallagher and Desjardins, 2007) by TECAN Multichannel Photometer, and manually equilibrated to the same concentration (200 ng/µl) by adding necessary volumes of 0.1 M TE-8. Stock was kept at -20°C, while working dilution (50 ng/µl) was used for analysis.

2.2.1.2 Molecular Marker Selection and Polymerase Chain Reaction Analysis

Markers used for genotyping the 5AS consisted of 15 simple sequence repeat (SSR), eleven transposable element based (TE-based), seven single nucleotide polymorphism (SNP), and two insertion site-based polymorphism (ISBP) markers. All 5AS specific markers were selected according to previous publications (Table 1).

Before genotyping the populations, markers were tested for: (i) their location on the 5A and (ii) fragments sizes. Information on physical position of markers was acquired by performing a polymerase chain reaction (PCR) on CS aneuploid lines CS-N5AT5B (Sears, 1966) and CS-DT5AL (Sears and Sears, 1978), and cytogenetic CS deletion lines C-5AS1-0.40, 5AS1-0.40-0.75, and 5AS3-0.75-0.97 (Endo and Gill, 1996). N5AT5B defined the markers on the 5A chromosome, DT5AL on the 5A short arm, while cytogenetic lines positioned markers in four different bins covering 40, 75, 97, and >97% of the 5AS from the centromere. Moreover, all 35 5A-specific markers that were used were subjected to a PCR on (non-irradiated) NIL3 line, and separated on 12% polyacrylamide-gels in order to identify fragments sizes, which facilitated marker combination in multiplex PCR. Obtained amplicons were later used as size markers.

Fourteen molecular markers (*BE426161*, *barc117*, *barc56*, *cfa2250*, *gpg1994*, *gpg2049*, *gpg2072, gpg2121*, *gwm129*, *gwm293*, *gwm304*, *gwm415*, *ldk215*, and *ldk49*), spread across the short arm of 5A, identified 28 informative lines in the Del-NIL3 panel. These lines constructed a subpanel that was further characterised with additional 21 molecular markers. Informative line, in this case, contains deletion for at least one 5AS specific marker. Therewithal, 274 CS-RH lines were screened with all 35 markers, pinpointing 40 informative lines. To confirm presence/absence of centromere, on both sub-panels three markers specific for the 5A long arm were tested.

Finally, 28 informative lines from the Del-NIL3 panel and 40 lines from the CS-RH were additionally verified by repeating PCR with all markers.

Both panels were screened with genetic markers utilizing optimized multiplex PCR (Henegariu et al., 1997). The primers used for amplification are listed in Table 1. Apart from the marker specificity for 5A chromosome, following criteria must have been met: (i) PCR products of markers intended for multiplex PCR must have different sizes, and (ii) at least one primer used in the multiplex should bear additional band(s) during the amplification in order to confirm efficacy of PCR in case of a deletion (a missing band). For markers that had only one amplicon, and could not have been combined with other

markers due to the band size, additional marker was used that was positioned either on 5A long arm, e.g. *wmc705-5A*, located in 5AL12-0.35-0.78 bin (Somers and Isaac, 2004), or some other chromosome, such as *umn10* (Liu et al., 2008) or *wmc75-5B* (Somers and Isaac, 2004).

PCR was performed in 384 wells PCR plates with a final volume of 10 µl. Each reaction contained 2 µl of the template DNA (50 ng/µl) and 8 µl of master mixture: 1x PCR buffer (including 1,5 mM $MgCl_2$), 0.2 mM of deoxynucleoside triphosphates, 0.36 µM FAM or Cy5-labelled 16-bp M13 primer (5' CCCAGTCACGACGTTG 3') (Oetting et al., 1995; Schuelke, 2000), 0.2 µM first M13-tailed reverse primer, 0.02 µM first forward primer, 0.2 µM second M13-tailed reverse primer, 0.02 µM second forward primer, and 1 U *Taq* polymerase. Samples were subjected to hot start touchdown PCR (Don et al., 1991), with the following parameters: (1) Predenaturation at 94°C for 4 minutes continued with (2) seven touchdown cycles, consisting of (2a) DNA denaturation at 94°C for 50 seconds, (2b) one minute of annealing, starting at 65°C in the first cycle and decrementing the temperature by 2°C every further cycle, and (2c) 60 seconds of elongation at 72°C; following (3) twenty-five cycles (denaturation at 94°C for 30 seconds, annealing at 51°C for 30 seconds, and elongation at 72°C for 30 seconds) were completed by the (4) final postextension step for 5 minutes at 72°C. Two-microliter aliquots of PCR products were separated on a 12% polyacrylamide gel by electrophoresis (400 V for 2 hours) in 1x TBE. Fragments were visualised by the Typhoon Trio gel image scanner. Scanning at 520 nm detected FAM, and at 670 nm detected Cy5 labelled fragments.

Table 1 *List of molecular markers used for fine mapping*

Locus	Type	PCR primers		Reference	5A bin according to literature
barc56-5A	SSR[3]	F[1] R[2]	GCGGGAATTTACGGGAAGTCAAGAA GCGAGTGGTTCAAATTTATGTCTGT	(Somers et al., 2004)	5AS3-0.75-0.98
barc117-5A	SSR	F R	TCATGCGTGCTAAGTGCTAA GAGGGCAGGAAAAAGTGACT	(Somers et al., 2004)	5AS3-0.75-0.98
barc186-5A	SSR	F R	GGAGTGTCGAGATGATGTGGAAAC CGCAGACGTCAGCAGCTCGAGAGG	(Somers et al., 2004)	C-5AL12-0.35 5AL17-0.78-0.87
BE425161-5A	SNP[4]	F R	GGATGGTTCTGACCCAATATG ATCATGCCGACAAACAGCTT	(Akhunov et al., 2010)	C-5AS1-0.40
BE444720-5A	SNP	F R	GCCCTCGAGAAGATGTTCAG GAGCATTAACAGTAACTCGGG	(Akhunov et al., 2010)	5AS3-0.75-0.98
cfa2250-5A	SSR	F R	AGCCATAGATGGCCCTACCT CACTCAATGGCAGGTCCTTT	(Sourdille et al., 2001) (Somers et al., 2004)	C-5AS1-0.40
gpg277	TE-based[5]	F R	TCCATGTTGTCTTCAACCCA TCCAAGTAGAGACCCATCCG	(Barabaschi et al., 2015)	5AS1-0.40-0.75
gpg1321	TE-based	F R	CCATCGATCTTAGACGCACA ATTGCTCTACGTGGTGCATG	(Barabaschi et al., 2015)	C-5AS1-0.40
gpg1994	ISBP[6]	F R	GGTGGAGGAATGTTCACAGG CACCGTTTGCGATTATTGTG	(Barabaschi et al., 2015)	5AS1-0.40-0.75
gpg2034	TE-based	F R	CCTCCTGGCGAGCAGATAT TTATCCACCATTGGTCCGTT	(Barabaschi et al., 2015)	C-5AS1-0.40
gpg2049	TE-based	F R	GGCCAAAGAAAGCTTATCCC CCAGTGAACCGTCTGCTGTA	(Barabaschi et al., 2015)	5AS1-0.40-0.75
gpg2072	TE-based	F R	TCCGAGTGACCTGTATGCTG AATCCATGCTTCCCTCTGTG	(Barabaschi et al., 2015)	5AS1-0.40-0.75
gpg2083	TE-based	F R	TTAGTTCAATGGCAGGTCGA CCATCTCTTCGCCGAACTAG	(Barabaschi et al., 2015)	C-5AS1-0.40
gpg2121	TE-based	F R	TGCTTGTTCTTGCTCCAATG GGCCACCTTGCTACACATCT	(Barabaschi et al., 2015)	C-5AS1-0.40
gpg2162	TE-based	F R	AAGATCAAATGGCCCTTCCT GGCTATGCATGGTCCAATCT	(Barabaschi et al., 2015)	5AS3-0.75-0.97
gpg2232	ISBP	F R	CGATTAAGAGCGATAATCAACCA TAAGAGACCGTTTTGGCCTG	(Barabaschi et al., 2015)	C-5AS1-0.40
gpg2233	TE-based	F R	GTCGACGTTCACATGACACC TGGTCTTCCACCACTTGTCC	(Barabaschi et al., 2015)	5AS1-0.40-0.75
gpg2326	TE-based	F R	CAGCGTCAGTCCGGATTAGT TCTAATTCTTCGGCGACGAT	(Barabaschi et al., 2015)	C-5AS1-0.40

Continuation from the previous page

Locus	Type	PCR primers		Reference	5A bin according to literature
gwm129-5A	SSR	F	TCAGTGGGCAAGCTACACAG	(Röder et al., 1998)	C-5AS1-0.40
		R	AAAACTTAGTAGCCGCGT		
gwm293-5A	SSR	F	TACTGGTTCACATTGGTGCG	(Röder et al., 1998) (Somers et al., 2004)	5AS1-0.40-0.75
		R	TCGCCATCACTCGTTCAAG		
gwm304-5A	SSR	F	AGGAAACAGAAATATCGCGG	(Röder et al., 1998) (Somers et al., 2004)	C-5AS1-0.40
		R	AGGACTGTGGGGAATGAATG		
gwm415-5A	SSR	F	GATCTCCCATGTCCGCC	(Röder et al., 1998) (Somers et al., 2004)	C-5AS1-0.40
		R	CGACAGTCGTCACTTGCCTA		
iwb8393	SNP	F	ACCGAAATAGGATTTGCCTCAT	(Wang et al., 2014)	5AS1-0.40-0.75
		R	TGCTTATCTTGATGGCCACA		
iwb11440	SNP	F	CCGATTATTTGCCTTGCGTTTTTAC	(Wang et al., 2014)	5AS3-0.75-0.97
		R	AGCGTCGTGAAATCTGTC		
iwb58275	SNP	F	ATATAGTGAGTTGGAAGGGCAG	(Wang et al., 2014)	5AS1-0.40-0.75
		R	GTGAAGCTGATGGGAAGAAG		
iwb62899	SNP	F	TGCTATGGCTATACTACGGC	(Wang et al., 2014)	5AS3-0.75-0.97
		R	GCGCCGAAGCCATTGACT		
iwb75561	SNP	F	TGGCATTCCTTACCTATTTGCG	(Wang et al., 2014)	5AS1-0.40-0.75
		R	CTAGTGGATGGGTGTTCACAT		
jfio2	TE-based	F	ACGCTGGAGACGTATCACTGT	(Barabaschi et al., 2015)	C-5AS1-0.40
		R	GGTGTCCTTCCTGATCTCCA		
ldk2	SSR	F	ATCAGGTCCACACACCACAC	(Barabaschi et al., 2015)	5AS1-0.40-0.75
		R	AATCCACGAAGACGCTATCC		
ldk14	SSR	F	TTTCTGTTTTGCCTCTGGAAA	(Barabaschi et al., 2015)	5AS1-0.40-0.75
		R	GGGCCTTTCCCTTTTGTTTT		
ldk49	SSR	F	TCCACACACCACACACACAC	(Barabaschi et al., 2015)	5AS1-0.40-0.75
		R	AGACGCTATCCGATCCTCTG		
ldk113	SSR	F	CACTGCTCCACCACAGC	(Barabaschi et al., 2015)	C-5AS1-0.40
		R	GCGAAGGGTTAAACCGTAAAC		
ldk215	SSR	F	CTGAGCTGAAGCAAGACAcg	(Barabaschi et al., 2015)	C-5AS1-0.40
		R	CGGGCATCTTCTCTACATCG		
ldk267	SSR	F	AATTAGCAGACCGCATGTACG	(Barabaschi et al., 2015)	5AS3-0.75-0.97
		R	TCCAAGTTGAGAGCTGATGG		
wmc150-5A	SSR	F	CATTGATTGAACAGTTGAAGAA	(Somers et al., 2003)	5AS1-0.40-0.75
		R	CTCAAAGCAACAGAAAAGTAAA		

[1] F – Forward primer
[2] R – Reverse primer
[3] SSR – Single Sequence Repeats
[4] SNP – Single Nucleotide Polymorphism
[5] TE-based – Transposable Elements based
[6] ISBP – Insertion Site-Based Polymorphism

2.2.1.3 Marker Analysis

Samples from each plate were compared to (i) primer specific size markers, (iii) amplicons of wild type NIL3, and (iii) amplicons of Chinese Spring aneuploid lines, nullitetrasomic line N5AT5B (Sears, 1966) and ditelosomic DT5AL (Sears and Sears, 1978).

Scoring was carried out in Photoshop by assigning (i) **1** for presence of a fragment, (ii) **d** for absence, i.e. deletion, (iii) **m** for a missing value, i.e. PCR failure, (iv) **x** for unintelligible results, and (v) **e** for negative control (Figure 5).

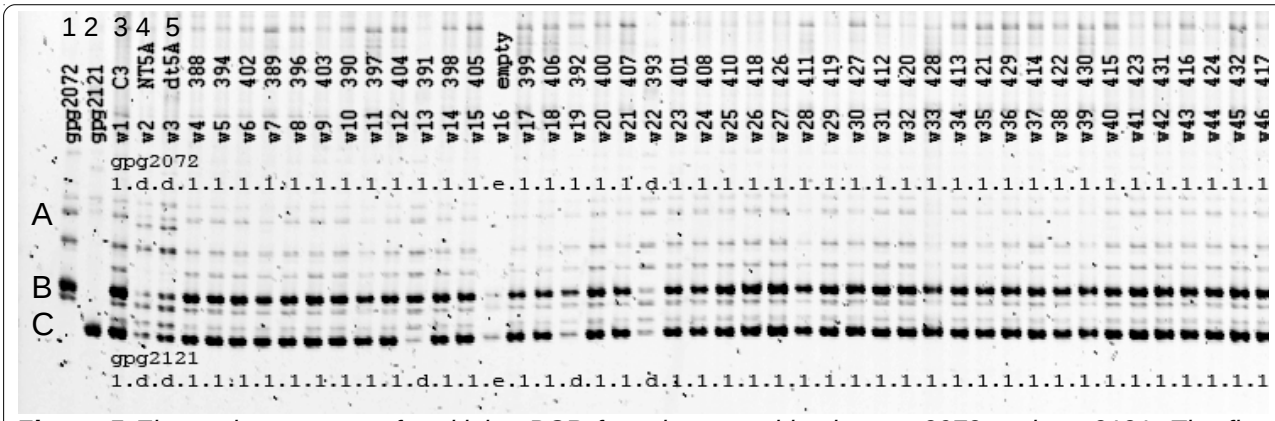

Figure 5 *Electrophoretogram of multiplex PCR for primer combination gpg2072 and gpg2121. The first two columns are size markers for gpg2072 and gpg2121. Third column are amplicons for the C3 with this primer combination, followed by the N5AT5B in the fourth, and dt5AL in the fifth column. Gpg2072 amplifies two non 5AS specific sequences (A), and two sequences on 5AS (B), while gpg2121 amplifies only 5AS specific sequence (C). Each marker was evaluated by assigning 1 for the present fragment, d for the absent fragment (deletion), m for a missing value (i.e. PCR failure), x for unintelligible results, and e for the negative control.*

2.2.2 Assembling the map

Maps for CS-RH, Del-NIL3, and consensus map were generated in the open-source CarthaGène 1.2-LKH program (de Givry et al., 2005). Maps were created separately for each population, and a consensus map was calculated using information from both populations. Del-NIL3 and CS-RH maps were calculated with the algorithm for a haploid model. Datasets of populations Del-NIL3 and CS-RH were merged by the command *dsmergen*. Marker association with the 5AS was already known, thus all markers were taken together as a single linkage group. Markers with the same deletion/retention patterns were merged to single markers. Initially, markers were ordered using two-points log-likelihood (LOD) by running the *lkh* commands (*lkh, lkhn, lkhl, lkhd*). This converted the

given marker data into a Travelling Salesman Problem using the Lin-Kernighan heuristic (Lin and Kernighan, 1973). Executing *polish* and *flips* commands provided a map with improved LOD. In the following step, the Del-NIL3 and the CS-RH datasets were merged by the command *dsmergor*, producing consensus data sets sharing marker order, but separate parameter estimated with per-data-set distances. Marker order for the combined analysis of both populations was derived from the marker order of the best previously calculated map, with following tuning by *polish* and *flips* commands. Algorithm for the diploid model for both populations separately (*dsmergor*) and for the consensus population (*dsmergen*) determined the distances between markers in centiRays (cR) for Del-NIL3 and CS-RH.

Visual representation for each map was created in the MapChart, version 2.3.

2.2.1 Characterizing the Del-NIL3 and CS-RH populations

To facilitate data processing, such as an estimation of the total number of deletions and obligate breaks, deletion and retention frequency and finally size of the deletions, all the data from the marker analysis was arranged in map order for each line (Table 2 and Table 4).

Del-NIL3 and CS-RH populations were characterised for: (i) the number of obligate breaks per line and per marker, (ii) the number of interstitial and terminal deletions, (iii) the retention frequency for individual marker, and (iv) the retention frequency of each line.

Obligate breaks were counted for each line, where an obligate break refers to a subsequent presence and absence, or absence and presence of two adjacent markers in a given map order (Kalavacharla, 2006). One obligate break produces a terminal deletion that causes the loss of the fragment distal to the break, while two consecutive obligate breaks are necessary for an interstitial deletion (Griffiths et al., 2000).

The deletion frequency for each line was calculated as a percentage of markers deleted out of all tested markers. By subtracting the deletion frequency of each line from 100, the retention frequency was calculated, which indicates the proportion of a chromosome that is retained after irradiation (Mazaheri et al., 2015).

The retention frequency for each marker was calculated as percentage of marker retained across the population. Interestingly, marker *wmc150* amplified two bands at the different locations along the 5A short arm in both panels, thus each amplicon was evaluated separately and calculated as an individual marker (*wmc150a* and *wmc150b)*.

2.2.2 Estimating the Sizes of Deletions

A single deletion was characterized as a deletion of either a single marker or of a continuous loss of markers located next to each other. To estimate the size of each deletion in cR, average of minimum and maximum deletion size was taken. Minimum size of a deletion is the difference between the cumulative distances acquired by the CarthaGene of the most distal and the most proximal deleted marker, while maximum size of a deletion is the difference between the cumulative distances of the most distal and the most proximal retained marker. Map distances were converted into physical distances (Mbp) using the ratio of physical and map distances (0.66 Mbp/cR for Del-NIL3 and 0.99 Mbp/cR for the CS-RH panel) (Table 3 and Table 5). The DNA content of the 5AS is estimated at 295 Mbp (Kumar et al., 2007; Paux et al., 2008), meaning that C-5AS1-0.40 has an approximate size of 118 Mbp, 5AS1-0.40-0.75 103.25 Mbp and 5AS3-0.75-0.97 64.9 Mbp (Kumar et al., 2007).

3 RESULTS

Overall, 1764 Del-NIL3 lines were preliminary screened with 14 markers and 276 CS-RH lines with 35 5AS specific markers, that identified 28 and 40 informative lines, respectively. Informative lines from both panels were genotyped with 35 markers. Results of both panels positioned nine molecular markers in the bin farthest from the centromere, 5AS3-0.75-0.97, 13 markers in the 5AS1-0.40-0.75, and 13 in the bin closest to the centromere C-5AS1-0.40.

3.1 Deletion Population of Near Isogenic Lines (Del-NIL3)

3.1.1 Characterization of the Selected Del-NIL3 panel

Fourteen markers tested on 1764 NILs distinguished 28 informative lines featuring deletions in the 5AS6-0.97 region (*cfa2250* – *IWB11440*). Informative lines were further characterized with totally 35 markers. As seen in Table 2, informative lines formed 23 haplotypes. Based on the 35 mapped markers, a total of 49 obligate breaks generated five terminal and 22 interstitial deletions on the short arm of the 5A chromosome.

Of the 28 informative lines, two lines (D_723 and D_393) completely missed the 5A short arm. Line D_627 had two separate fragments deleted, while the remaining lines showed a single fragment deleted. Altogether, six lines showed a loss of a single marker.

Deletions were observed along the whole short arm. Retention frequency for each marker across the informative lines reveals variations in marker retention along the length of chromosome 5A, ranging from 64.29 to 92.86% (Table 2). Most markers had a retention frequency between 70 and 80% (Figure 6a). The average marker retention among informative lines was 74.9%. Results demonstrate uneven distribution of marker loss. Average marker retention per bin slightly decreased with the increasing distance from the centromere, 76.65, 74.74, and 72.58% for C-5AS1-0.40, 5AS1-0.40-0.75, and 5AS3-0.75-0.97, respectively. Number of obligate breaks per bin was 8, 19, and 22 per 5AS3-0.75-0.97, 5AS1-0.40-0.75, and C-5AS1-0.40, respectively. Considering the physical length of

the bins, the number of breaks per distance are similar.

Retention frequency for each line varied from 0 to 97.22% (Table 3). In Figure 6b it is presented on a scale from zero to 99%, with zero meaning complete elimination of the short arm of the 5A chromosome, and one indicating no deletions on the same interval.

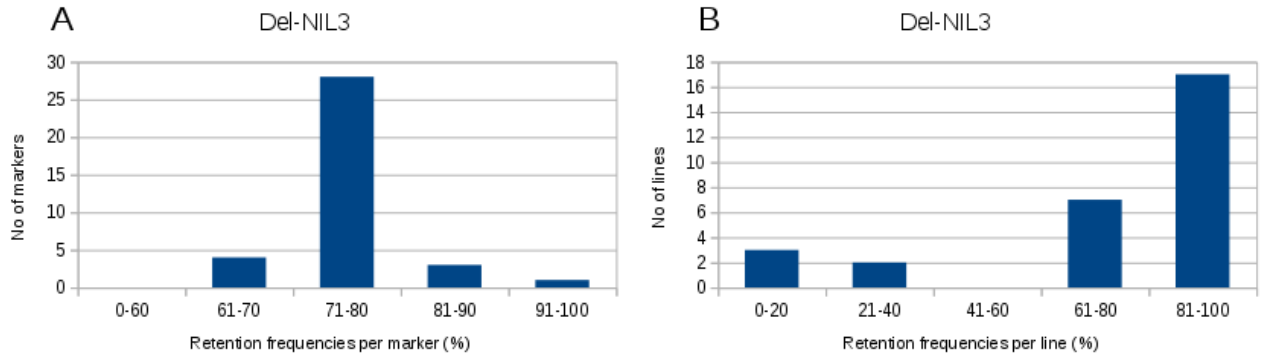

Figure 6 *Retention frequencies per marker and per line for Del-NIL3 population. In both charts, x-axis represents percentages, and y-axis number of lines. In seed irradiated panel most markers are retained between 70 and 85%, and most lines have retention frequencies between 80 and 99%.*

3.1.2 Generating a Comprehensive Map

Del-NIL3 map was generated from the genotypic data from 35 molecular markers. Markers were mapped to 27 unique positions on the 5AS, and covered the distance of 433.3 cR (Figure 7).

Resolution is one of the most important characteristics of a map, and it is defined as the minimum physical distance between two marker loci necessary to map them at separate positions (Kalavacharla, 2006). Assuming even distribution of obligate breaks along the chromosome arm, the average distance between two adjacent marker loci was 16.04 cR (433.3 cR/27 loci). The short arm of the 5A chromosome is 295 Mbp in length, nevertheless the used deletion stocks together cover 97% (286.15 Mb) of the short arm of the 5A chromosome. The resolution can be expressed as the ratio between physical and map distances (i.e. Mbp/cR or Mbp/cM) (Kumar et al., 2012). The overall resolution of the map was 0.66 Mbp/cR (286.15 Mbp/433.3 cR). The physical to genetic distance ratios per bin were 0.6 Mbp/cR for C-5AS1-0.40, 0.59 Mbp/cR for 5AS1-0.40-0.75, and 1.02 Mbp/cR for 5AS3-0.75-0.97 (Table 2).

Table 2 *Marker data for 28 informative lines in Del-NIL3. Marker data shows overall marker arrangement and deletion positions for each line. On the left is given marker order on the 5AS, and their position in bins. Green fields (d) represent absent chromosome parts - deletions, yellow (1) present chromosome parts. Obligate breaks and retention frequency were calculated for each marker and per bin. Retention frequency per marker is presented by a colour scheme, red stands for lowest and green for the highest retention frequency. Distances between markers are given in cR and Mbp, and are accentuated with colours ranging from red (zero) to green (highest). Cumulative distance is given in cR. Resolution is a ratio of Mbp per cR and is calculated for each bin, and average.*

		D_723	D_393	D_1612	D_752	D_1303	D_725	D_391	D_175	D_451	D_573	D_291	D_457	D_515	D_479	D_1077	D_1268	D_1075	D_1988	D_1604	D_612	D_1494	D_1433	D_627	D_628	D_1537	D_473	D_164	D_426	Obligate breaks		Retention frequency		Distance between markers (cR)	Distance between markers (Mbp)	Cumulative distance (cR)	5AS = 295 Mbp/1C	Mb/cR
																													per marker	per bin	per marker	per bin					
5AS3-0.75-0.97	IWB11440	d	d	1	1	1	1	1	1	1	1	d	1	1	1	d	x	1	1	1	1	1	1	d	1	d	1	1	1	0		75.00				0		
	barc186	d	d	1	1	1	1	1	1	1	1	d	1	1	1	d	d	1	1	1	1	1	1	1	1	d	1	d	d	3		71.43		26.4	26.86	26.4		
	ldk267	d	d	1	1	1	1	1	1	1	1	d	1	1	1	d	x	1	1	1	1	1	1	1	1	d	1	d	d	0		71.43		0	0.00	26.5		
	gpg2326	d	d	1	1	1	1	1	1	1	1	d	1	1	1	d	d	1	1	1	1	1	1	1	1	d	1	d	d	0		71.43		0	0.00	26.5		
	IWB62899	d	d	1	1	-	1	1	1	1	1	d	1	1	1	d	d	1	1	1	1	1	1	1	1	d	1	d	1	1	8	75.00	72.62	7.1	7.22	33.6	64.9	1.02
	be444720	d	d	-	1	-	1	1	1	1	1	d	1	1	1	x	x	1	1	1	1	1	1	d	1	d	1	d	1	1		71.43		7.4	7.53	40.9		
	barc56	d	d	1	1	1	1	1	1	1	1	d	1	1	1	d	d	1	1	1	1	1	1	d	1	d	1	1	1	1		75.00		7.5	7.63	48.5		
	gpg2162	d	d	1	1	1	1	1	1	1	1	d	1	1	1	d	d	1	1	1	1	1	1	d	1	d	1	1	1	0		75.00		0	0.00	48.5		
	barc117	d	d	1	1	1	1	1	1	1	1	d	1	1	1	d	d	1	1	1	1	1	1	d	d	d	d	1	1	2		67.86		15.3	15.56	63.8		
5AS1-0.40-0.75	IWB75561	d	d	1	1	1	1	1	1	1	1	d	1	1	1	d	d	1	1	1	1	1	1	d	d	1	1	1	1	2		75.00		15.4	9.16	79.2		
	wmc150a	d	d	-	1	-	1	1	1	1	-	d	1	1	1	x	d	1	1	1	1	1	-	d	1	1	1	1	1	1		78.57		8	4.76	87.2		
	gwm293	d	d	1	1	1	1	1	1	1	1	d	1	1	1	d	d	1	1	1	1	1	1	d	1	1	1	1	1	0		78.57		0	0.00	87.2		
	gwm304	d	d	1	1	1	1	1	1	1	1	d	1	1	1	d	d	1	1	1	1	1	1	d	1	1	1	1	1	0		78.57		0	0.00	87.2		
	IWB8393	d	d	1	1	1	1	1	1	1	1	d	1	1	1	d	d	1	1	1	1	1	1	d	1	1	1	1	1	0		78.57		0	0.00	87.2		
	wmc150b	d	d	1	1	1	1	1	1	1	-	d	1	1	1	d	d	1	1	1	d	d	1	d	1	1	1	1	1	2		71.43		16.6	9.87	103.8		
	gpg2049	d	d	1	1	1	1	1	1	1	1	d	1	1	1	d	d	1	1	1	d	d	d	d	1	1	1	1	1	1	19	67.86	74.74	7.1	4.22	110.9	103.25	0.59
	ldk49	d	d	1	1	1	1	1	1	1	1	d	1	1	1	d	d	1	1	1	d	d	d	1	1	1	1	1	1	1		71.43		7.1	4.22	118		
	ldk2	d	d	1	1	-	1	1	1	1	1	d	1	1	1	d	x	1	1	1	x	d	d	1	1	-	1	1	1	0		71.43		0	0.00	118		
	gpg2233	d	d	1	1	1	1	1	1	1	1	d	1	1	1	d	d	1	1	1	d	d	1	1	1	1	1	1	1	1		75.00		7.6	4.52	125.6		
	gpg2072	d	d	1	1	1	1	1	1	1	1	d	1	1	1	d	d	1	1	1	d	1	1	1	1	1	1	1	1	1		78.57		8	4.76	133.7		
	IWB58275	d	d	1	1	1	1	1	1	1	1	d	1	1	1	d	x	1	1	1	d	-	-	1	1	1	1	1	1	0		78.57		0	0.00	133.7		
	gpg277	d	d	1	1	1	1	1	1	1	1	d	1	1	1	d	d	d	d	d	1	1	1	1	1	1	1	1	1	4		71.43		39.9	23.73	173.5		
	gpg1994	d	d	1	1	1	1	1	d	d	1	d	1	d	1	d	d	1	1	1	1	1	1	1	1	1	1	1	1	6		71.43		63.9	38.01	237.4		
C-5AS1-0.40	gwm129	d	d	1	1	d	1	1	d	d	1	d	1	d	d	1	1	1	1	1	1	1	1	1	1	1	1	1	1	4		71.43		35.7	21.50	273.1		
	ldk14	d	d	1	1	d	1	1	d	d	1	d	1	d	1	1	1	1	1	1	1	1	1	1	1	1	1	1	1	1		75.00		7.5	4.52	280.6		
	jfio2	d	d	1	1	d	1	1	d	d	1	d	1	d	1	1	1	1	1	1	1	1	1	1	1	1	1	1	1	0		75.00		0	0.00	280.6		
	gpg2232	d	d	1	1	d	1	1	d	d	1	d	d	1	1	-	1	1	1	1	1	1	1	1	1	1	1	1	1	2		75.00		16.7	10.06	297.3		
	gpg2083	d	d	-	1	x	1	1	d	d	d	d	d	1	1	-	-	-	-	1	1	1	-	1	1	1	1	1	1	1		71.43		7.6	4.58	305		
	gwm415	d	d	1	1	d	1	1	d	d	d	d	d	1	1	1	1	1	1	1	1	1	1	1	1	1	1	1	1	0		71.43		0	0.00	305		
	gpg2121	d	d	1	1	d	d	d	d	d	d	d	d	1	1	1	1	1	1	1	1	1	1	1	1	1	1	1	1	2	22	64.29	76.65	14.6	8.79	319.6	118	0.60
	ldk113	d	d	1	1	d	d	d	d	d	d	d	1	1	1	1	1	1	1	1	1	1	1	1	1	1	1	1	1	1		67.86		6.8	4.10	326.4		
	gpg1321	d	d	1	1	d	d	d	1	1	-	1	1	1	1	1	1	1	1	1	1	1	1	1	1	1	1	1	1	4		82.14		34.5	20.78	360.8		
	ldk215	d	d	d	1	x	d	d	1	1	1	1	1	1	1	-	-	1	1	1	1	1	1	1	1	1	1	1	1	1		78.57		10.5	6.32	371.4		
	gpg2034	d	d	d	1	d	1	1	1	1	1	1	1	1	1	1	1	1	1	1	1	1	1	1	1	1	1	1	1	2		85.71		19.4	11.69	390.7		
	be425161	d	d	d	d	1	1	1	1	1	1	1	1	1	1	1	1	1	1	1	1	1	1	1	1	1	1	1	1	2		85.71		20.3	12.23	411		
	cfa2250	d	d	1	1	1	1	1	1	1	1	1	1	1	1	1	1	1	1	1	1	1	1	1	1	1	1	1	1	2		92.86		22.3	13.43	433.3		
																													49		74.90			286.05		286.15	**0.66**

3.1.3 Size of Deletions in the Del-NIL3 Panel

Map distances were converted into physical distances (Mb) using the ratio of physical and map distances (0.66 Mbp/cR).

Average deletion size was 105.31 cR or 69.55 Mbp. The shortest deletion was 13.20 cR or 8.72 Mbp, while the longest covered 433.3 cR or 286.15 Mbp. As it is evident from Table 3, minimum retention frequency per line (0.0%) corresponds to the maximum deletion size (433.3 cR, i.e. 286.15 Mbp). Six lines had a single marker deleted and their maximum retention frequency was 97.22%, while calculated average deletion size (mean of maximum and minimum deletion sizes) in cR were from 15.35 (D_473), to 51.85 (D_1075, D_1604, D_1988). Although deletions that resulted in loss of a single marker have a calculated size, it is impossible to say with the given results whether those are true deletions or just SNPs.

Table 3 *Del-NIL3 population characterization and estimation of deletion sizes (in cR and Mbp)*

Line	Retention frequency	Obligate breaks	Deletion size (cR)			Deletion size (Mbp)		
			Maximum	Minimum	Average	Maximum	Minimum	Average
D_393	**0.00**	0	433.30	433.30	**433.30**	286.15	286.15	**286.15**
D_723	**0.00**	0	433.30	433.30	**433.30**	286.15	286.15	**286.15**
D_291	13.89	1	360.80	326.40	343.60	238.27	215.55	226.91
D_1077	36.11	1	273.10	237.40	255.25	180.35	156.78	168.57
D_1268	36.11	1	273.10	237.40	255.25	180.35	156.78	168.57
D_627	66.67	3	84.40	70.00	77.20	55.74	46.23	50.98
			26.40	0.00	**13.20**	17.43	0.00	**8.72**
D_1303	69.44	2	173.60	117.60	145.60	114.64	77.66	96.15
D_1537	75.00	1	79.20	63.80	71.50	52.30	42.13	47.22
D_175	75.00	2	187.30	89.00	138.15	123.69	58.78	91.23
D_451	75.00	2	187.30	89.00	138.15	123.69	58.78	91.23
D_612	80.56	2	86.30	29.90	58.10	56.99	19.75	38.37
D_1494	86.11	2	46.50	21.80	34.15	30.71	14.40	22.55
D_164	86.11	2	48.50	14.50	31.50	32.03	9.58	20.80
D_391	88.89	2	85.70	51.80	68.75	56.60	34.21	45.40
D_457	88.89	2	45.80	22.30	34.05	30.25	14.73	22.49
D_515	88.89	2	123.80	43.20	83.50	81.76	28.53	55.14
D_573	88.89	2	63.50	21.40	42.45	41.94	14.13	28.03
D_725	88.89	2	85.70	51.80	68.75	56.60	34.21	45.40
D_1433	91.67	2	21.80	7.10	14.45	14.40	4.69	9.54
D_1612	91.67	2	72.50	39.60	56.05	47.88	26.15	37.02
D_426	91.67	2	33.60	0.10	16.85	22.19	0.07	11.13
D_628	94.44	2	38.70	15.40	27.05	25.56	10.17	17.86
D_1075	**97.22**	2	103.70	0.00	51.85	68.48	0.00	34.24
D_1604	**97.22**	2	103.70	0.00	51.85	68.48	0.00	34.24
D_1988	**97.22**	2	103.70	0.00	51.85	68.48	0.00	34.24
D_473	**97.22**	2	30.70	0.00	15.35	20.27	0.00	10.14
D_479	**97.22**	2	43.20	0.00	21.60	28.53	0.00	14.26
D_752	**97.22**	2	42.60	0.00	21.30	28.13	0.00	14.07
	74.90	49	**127.30**	**83.31**	**105.31**	**84.07**	**55.02**	**69.55**

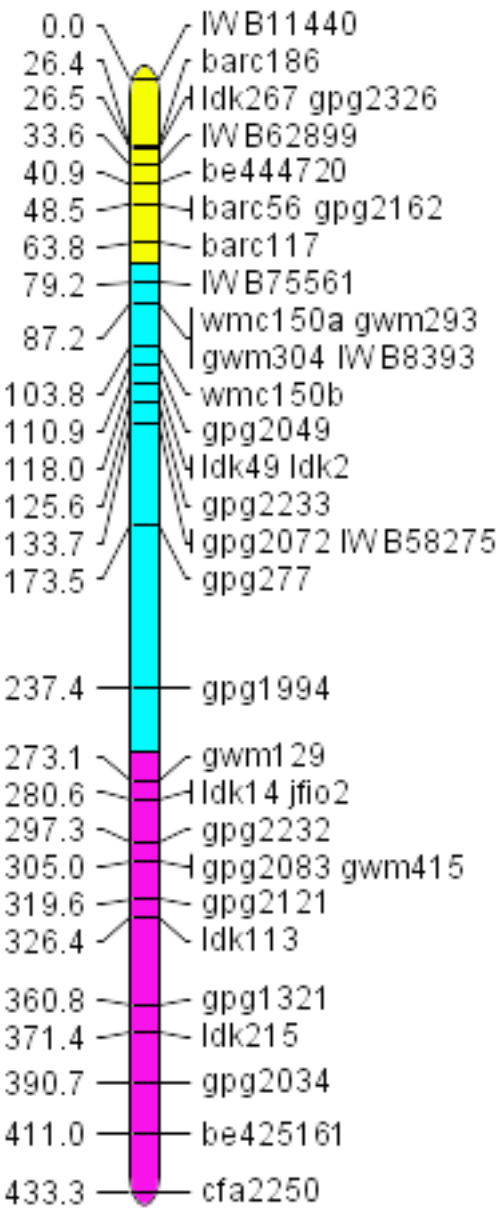

Figure 7 *Radiation induced deletion map of 5A chromosome short arm based on 25 makers and 28 informative lines created by seed irradiation. Bin are presented in different colours, C-5AS1-0.40 in magenta, 5AS1-0.40-0.75 in cyan, and 5AS3-0.75-0.97 in yellow. Map distances are reported in cR (left). Marker order for the Del-NIL3 map is on the right side.*

3.2 Chinese Spring Radiation Hybrid

3.2.1 Characterization of the Selected CS-RH Panel

Thirty-five 5AS specific markers that were used to survey the 274 CS-RH lines revealed 40 informative lines bearing the deletions on the 5AS, forming 29 haplotypes (Table 4). Radiation induced totally 58 obligate breaks in the examined region on the 5AS, causing 23 terminal and 18 interstitial deletions. Line CS_112 shows double deletion, while the rest show single deletion ranging from the loss of a single marker (CS_94, CS_97, CS_112, and CS_140) to almost the whole short arm (CS_75).

Retention frequency for markers among informative lines varied from 32.5 to 97.5%, with the average value of 52.99% (Figure 8a). As it is evident in the Del-NIL3 panel too, the retention frequency is not equally spread along the chromosome arm, with even greater difference among the bins, with values of 75.58, 40.89, and 39.17 for the C-5AS1-0.40, 5AS1-0.40-0.75, and 5AS3-0.75-0.97, respectively. Number of obligate breaks is 22, 25, and 11 for the C-5AS1-0.40, 5AS1-0.40-0.75, and 5AS3-0.75-0.97, respectively. Interestingly, the same interval *gpg277-gpg1994*, as in the Del-NIL3 panel, shows the most breaks (10). Retention frequency for each line ranged from 5.56 to 97.22, with average of 52.99 (Figure 8b).

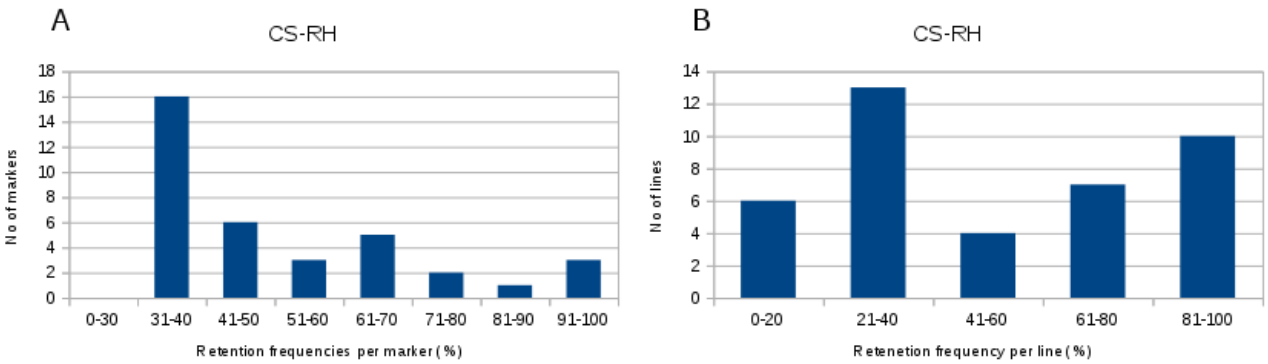

Figure 8 *Retention frequencies per marker and per line for CS-RH panel. In both charts, x-axis represents percentages, and y-axis number of lines. In pollen irradiated panel most markers are retained between 0 and 50%, and most lines have retention frequencies between 20 and 80%.*

3.2.2 Generating a Comprehensive Map

Thirty-five 5AS specific markers, used to analyse CS-RH panel, were delineated to 26 loci, covering the distance of 288.3 cR (Figure 9), thus the average distance between two loci is 11.08 cR (288.3 cR/26 loci). Average ratio of physical to map distances is 0.99 Mbp/cR (286.15 Mbp/288.33 cR), with 1.02 Mbp/cR for C-5AS1-0.40, 0.82 Mbp/cR for 5AS1-0.40-0.75, and 1.40 Mbp/cR for 5AS3-0.75-0.97.

3.2.3 Size of Deletions in the CS-RH Panel

The sizes of the deletion (Table 5) in the CS-RH panel were calculated the same way as for the Del-NIL3, except the multiplying factor that was used to convert to physical distances was 0.99 Mbp/cR.

The average retention frequency per line for this panel is 52.99, while average deletion size in cR is 123.98, thus 123.06 Mbp. Maximum retention frequency is 97.22 and it ranges from 10.95 cR (10.87 Mbp) to 40.15 cR (39.85 Mbp), whilst the smallest average deletion size is 10.3 cR (10.22 Mbp) for the line CS_112. Minimum retention frequency is 5.56, which corresponds to 282.55 cR or 280.44 Mbp.

Table 4 *Marker data for 40 informative lines in CS-RH. Marker data shows overall marker arrangement and deletion positions for each line. On the left is given marker order on the 5AS, and their position in bins. Green fields (d) represent absent chromosome parts - deletions, yellow (1) present chromosome parts. Obligate breaks and retention frequency were calculated for each marker and per bin. Retention frequency per marker is presented by a colour scheme, red stands for lowest and green for the highest retention frequency. Distances between markers are given in cR and Mbp, and are accentuated with colours ranging from red (zero) to green (highest). Cumulative distance is given in cR. Resolution is a ratio of Mbp per cR and is calculated for each bin, and average.*

		CS_212	CS_134	CS_75	CS_30	CS_93	CS_54	CS_141	CS_131	CS_140	CS_2	CS_163	CS_156	CS_9	CS_218	CS_168	CS_186	CS_25	CS_32	CS_52	CS_199	CS_73	CS_27	CS_117	CS_62	CS_67	CS_261	CS_94	CS_97	CS_120	CS_88	CS_118	CS_122	CS_247	CS_80	CS_262	CS_271	CS_4	CS_112	CS_81	CS_42	Obligate breaks		Retention frequency		Distance between markers (cR)	Distance between markers (Mbp)	Cumulative distance (cR)	5AS = 295 Mbp/1C	Mb/cR
																																										per marker	per bin	per marker	per bin							
5AS3-0.75-0.97	IWB11440	1	1	d	d	1	1	1	1	1	d	d	1	1	1	d	1	d	d	d	d	d	d	d	d	d	1	1	d	d	1	1	d	d	d	d	1	1	d		0		42.50				0			
	barc186	1	1	d	d	1	1	d	d	1	d	d	1	1	1	d	1	d	d	d	d	d	d	d	d	d	1	1	d	d	1	1	d	d	d	d	x	x	d	1	5		35.00		21.9	30.63	21.9			
	ldk267	1	1	d	x	1	1	d	d	1	x	d	1	1	1	d	1	x	d	d	d	d	d	d	d	d	1	1	x	d	-	1	d	d	x	d	d	d	d	1	0		35.00		0	0.00	21.9			
	gpg2326	1	1	d	d	1	1	d	d	1	d	d	1	1	1	d	1	d	d	d	d	d	d	d	d	d	1	1	d	d	1	1	d	d	d	x	d	d	1	1	1		37.50		3.9	5.45	25.8			
	IWB62899	1	1	d	x	1	1	d	d	1	d	d	-	-	1	x	1	d	d	d	d	d	d	d	d	d	1	1	d	d	1	1	d	d	d	d	d	d	1	1	0	11	37.50	39.17	0	0.00	25.8	64.9	1.40	
	be444720	1	1	d	d	1	1	x	x	1	d	d	-	1	1	d	1	d	d	d	d	d	d	d	d	d	1	1	d	d	1	1	d	d	d	x	d	d	1	1	0		37.50		0	0.00	25.8			
	barc56	-	1	d	d	1	1	d	d	1	d	d	1	1	1	d	1	d	d	d	d	d	d	d	d	d	1	1	d	d	1	1	d	d	d	1	1	1	1	1	3		45.00		12.6	17.62	38.4			
	gpg2162	1	1	d	d	d	1	d	d	1	d	d	1	1	1	d	1	d	d	d	d	d	d	d	d	d	1	1	d	d	1	1	d	d	d	1	1	1	1	1	1		42.50		4	5.59	42.4			
	barc117	1	1	d	d	d	d	d	d	1	d	d	1	1	1	d	1	d	d	d	d	d	d	d	d	d	1	1	d	d	1	1	d	d	d	1	1	1	1	1	1		40.00		4	5.59	46.4			
5AS1-0.40-0.75	IWB75561	1	1	d	d	d	d	d	d	1	x	d	1	1	1	d	1	d	d	d	d	d	x	d	d	d	d	1	1	d	d	d	d	d	d	d	1	1	d	1	1	3		32.50		12.5	10.24	58.8			
	wmc150a	1	1	d	d	d	d	d	d	1	d	d	1	1	1	d	1	d	d	d	d	d	x	d	d	d	d	1	1	d	d	d	d	d	d	d	1	-	1	1	1	2		37.50		8.1	6.64	67			
	gwm293	1	1	d	d	d	d	d	d	1	d	d	1	1	1	x	1	d	d	x	d	d	d	d	x	x	d	1	1	d	d	d	d	d	d	d	1	1	1	1	1	0		37.50		0	0.00	67			
	gwm304	1	1	d	d	d	d	d	d	1	d	d	1	1	1	d	1	d	d	d	d	d	d	d	d	d	d	1	1	d	d	d	d	d	d	1	1	-	1	1	1	1		40.00		4	3.28	71			
	IWB8393	1	1	d	d	d	d	d	d	1	d	d	d	1	1	d	1	d	d	d	d	d	d	d	d	d	d	1	1	d	d	d	d	1	1	1	-	1	1	1	1	2		40.00		8.3	6.80	79.3			
	wmc150b	1	1	d	d	d	d	d	d	1	d	d	d	1	1	d	1	d	d	d	d	d	d	d	d	d	d	1	1	d	d	d	d	1	1	1	1	1	1	1	1	0		40.00		0	0.00	79.3			
	gpg2049	1	1	d	d	d	d	d	d	1	d	d	d	1	1	d	1	d	d	d	d	d	d	d	d	d	d	1	1	d	d	d	d	1	1	1	1	1	1	1	1	0	25	40.00	40.89	0	0.00	79.3	103.25	0.82	
	ldk49	1	1	d	d	d	d	d	d	1	d	d	d	1	1	d	1	d	d	d	d	d	d	d	d	d	d	1	1	d	d	d	x	1	-	1	1	1	1	1	1	0		40.00		0	0.00	79.4			
	ldk2	1	1	d	d	d	d	d	d	1	x	d	d	1	1	d	1	d	d	d	x	d	x	d	d	d	d	1	1	d	d	d	d	1	1	-	1	1	1	1	1	0		40.00		0	0.00	79.4			
	gpg2233	1	1	d	d	d	d	d	d	1	d	d	d	1	1	d	1	d	d	d	d	d	d	d	d	d	d	1	1	x	d	d	d	1	1	1	1	1	1	1	1	0		40.00		0	0.00	79.4			
	gpg2072	1	1	d	d	d	d	d	d	1	d	d	d	1	1	d	1	d	d	d	d	d	d	d	d	d	x	1	1	d	d	d	1	1	1	-	-	1	1	1	1	1		42.50		4.1	3.36	83.5			
	IWB58275	d	-	d	d	x	d	d	x	1	d	d	x	1	1	d	1	d	d	d	d	d	d	x	d	d	d	1	1	d	d	1	1	-	1	1	1	1	-	1	1	2		42.50		8.7	7.13	92.1			
	gpg277	d	1	d	d	d	d	d	d	1	d	d	d	1	1	d	1	d	x	d	d	d	d	d	d	d	d	d	1	1	1	1	1	1	1	1	1	1	1	1	1	4		42.50		18.5	15.16	110.6			
	gpg1994	d	1	d	d	d	d	d	d	1	d	d	d	d	d	d	1	d	d	d	d	1	1	1	1	1	1	1	1	1	1	1	1	1	1	1	1	1	1	1	1	1	10		57.50		61.8	50.64	172.4			
C-5AS1-0.40	gwm129	d	d	d	d	d	d	d	d	1	d	d	d	d	d	d	d	d	1	1	1	1	-	1	1	1	1	1	1	1	1	1	1	1	1	1	-	1	1	1	1	5		60.00		25.9	26.37	198.2			
	ldk14	d	d	d	d	d	d	d	d	1	d	d	d	d	d	d	d	d	1	-	1	1	1	1	1	1	1	1	1	1	1	1	1	1	1	1	1	-	1	1	1	1	0		60.00		0	0.00	198.2			
	jfio2	d	d	d	d	d	d	d	d	1	d	d	d	x	d	d	1	1	1	1	1	1	1	1	1	1	1	1	1	1	1	1	1	1	1	1	1	1	1	1	1	2		65.00		9.5	9.67	207.7			
	gpg2232	d	d	d	d	d	d	d	d	1	d	x	d	x	d	1	1	1	1	1	1	1	1	1	1	1	1	1	1	1	1	1	1	1	1	1	-	1	1	1	1	1		67.50		4.6	4.68	212.3			
	gpg2083	d	d	d	d	d	d	d	d	1	d	d	d	d	d	1	1	1	1	1	1	1	1	1	1	1	1	1	1	1	1	1	1	1	1	1	1	1	1	1	1	0		67.50	--	0	0.00	212.4	--		
	gwm415	d	d	d	d	d	d	d	d	1	d	d	d	d	1	1	1	1	1	1	1	1	1	1	1	1	1	1	1	1	1	1	1	1	1	1	1	1	1	1	1	1		70.00		4.7	4.79	217			
	gpg2121	d	d	d	d	d	d	d	d	1	d	d	d	d	1	1	1	1	1	1	1	1	1	1	-	1	1	1	1	1	1	1	1	-	-	1	1	1	1	0	22	70.00	75.58	0	0.00	217.1	118	1.02	
	ldk113	x	d	d	d	d	d	d	d	1	d	d	d	1	1	-	1	-	1	1	1	1	1	1	1	1	1	1	1	1	1	1	1	1	1	1	1	1	1	1	1	1		72.50		4.8	4.89	221.9			
	gpg1321	x	d	d	d	d	d	d	d	d	1	1	1	1	1	1	1	1	1	1	1	1	1	1	1	1	1	1	1	1	1	1	1	1	1	1	1	1	1	1	1	4		77.50		21.9	22.30	243.8			
	ldk215	d	d	d	d	d	d	1	1	1	1	1	1	1	1	1	1	1	1	1	1	1	1	1	1	1	1	1	1	1	1	1	1	1	1	1	1	1	1	1	1	3		85.00		16.2	16.49	260			
	gpg2034	d	d	d	1	1	1	1	1	1	1	1	1	1	1	1	1	-	1	1	1	1	1	1	1	1	1	1	1	1	1	1	1	1	1	1	1	1	1	1	1	3		92.50		16.8	17.10	276.8			
	be425161	d	1	1	1	1	1	1	1	1	1	1	1	1	1	1	1	1	1	1	1	1	1	1	-	1	1	1	1	1	1	1	-	-	1	1	1	1	2		97.50		11.5	11.71	288.3			
	cfa2250	d	1	1	1	1	1	1	1	1	1	1	1	1	1	1	1	1	1	1	1	1	1	1	1	1	1	1	1	1	1	1	-	1	1	1	1	1	0		97.50		0	0.00	288.3			
																																									58		52.99			286.15		286.15	**0.99**

Table 5 *CS-RH population characterization and estimation of deletion sizes (in cR and Mbp)*

Line	Retention frequency	Obligate breaks	Deletion size (cR)			Deletion size (Mbp)		
			Maximum	Minimum	Average	Maximum	Minimum	Average
CS_75	**5.56**	1	288.30	276.80	**282.55**	286.15	274.74	**280.44**
CS_30	8.33	1	276.80	260.00	268.40	274.74	258.06	266.40
CS_131	13.89	2	260.00	221.90	240.95	258.06	220.25	239.15
CS_141	13.89	2	260.00	221.90	240.95	258.06	220.25	239.15
CS_163	13.89	1	243.80	221.90	232.85	241.98	220.25	231.11
CS_2	13.89	1	243.80	221.90	232.85	241.98	220.25	231.11
CS_168	27.78	1	212.30	207.70	210.00	210.72	206.15	208.43
CS_93	27.78	2	238.40	213.60	226.00	236.62	212.01	224.31
CS_25	30.56	1	207.70	198.20	202.95	206.15	196.72	201.44
CS_54	30.56	2	234.40	213.60	224.00	232.65	212.01	222.33
CS_199	36.11	1	198.20	172.40	185.30	196.72	171.11	183.92
CS_32	36.11	1	198.20	172.40	185.30	196.72	171.11	183.92
CS_52	36.11	1	198.20	172.40	185.30	196.72	171.11	183.92
CS_117	38.89	1	172.40	110.60	141.50	171.11	109.78	140.44
CS_261	38.89	1	172.40	110.60	141.50	171.11	109.78	140.44
CS_27	38.89	1	172.40	110.60	141.50	171.11	109.78	140.44
CS_62	38.89	1	172.40	110.60	141.50	171.11	109.78	140.44
CS_67	38.89	1	172.40	110.60	141.50	171.11	109.78	140.44
CS_73	38.89	1	172.40	110.60	141.50	171.11	109.78	140.44
CS_120	41.67	1	110.60	92.10	101.35	109.78	91.41	100.59
CS_88	41.67	1	110.60	92.10	101.35	109.78	91.41	100.59
CS_156	50.00	2	172.80	142.60	157.70	171.51	141.54	156.52
CS_212	55.56	1	204.80	196.20	200.50	203.27	194.74	199.00
CS_247	63.89	1	79.30	71.00	75.15	78.71	70.47	74.59
CS_80	66.67	1	71.00	67.00	69.00	70.47	66.50	68.49
CS_118	69.44	2	45.70	24.70	35.20	45.36	24.52	34.94
CS_134	69.44	2	115.90	78.60	97.25	115.04	78.01	96.52
CS_122	72.22	2	37.10	20.60	28.85	36.82	20.45	28.63
CS_262	72.22	1	67.00	58.80	62.90	66.50	58.36	62.43
CS_9	77.78	2	111.30	44.70	78.00	110.47	44.37	77.42
CS_112	83.33	4	20.60	0.00	**10.30**	20.45	0.00	**10.22**
			38.40	3.90	20.97	38.11	3.87	20.81
CS_218	83.33	2	106.40	40.00	73.20	105.61	39.70	72.65
CS_271	83.33	1	38.40	25.80	32.10	38.11	25.61	31.86
CS_4	83.33	1	38.40	25.80	32.10	38.11	25.61	31.86
CS_186	94.44	2	35.30	0.00	17.65	35.04	0.00	17.52
CS_81	94.44	2	25.80	0.00	12.90	25.61	0.00	12.80
CS_140	**97.22**	2	38.10	0.00	19.05	37.82	0.00	18.91
CS_42	**97.22**	1	21.90	0.00	10.95	21.74	0.00	10.87
CS_94	**97.22**	2	80.30	0.00	40.15	79.70	0.00	39.85
CS_97	**97.22**	2	80.30	0.00	40.15	79.70	0.00	39.85
	52.99	58	**140.11**	**107.86**	**123.98**	**139.06**	**107.05**	**123.06**

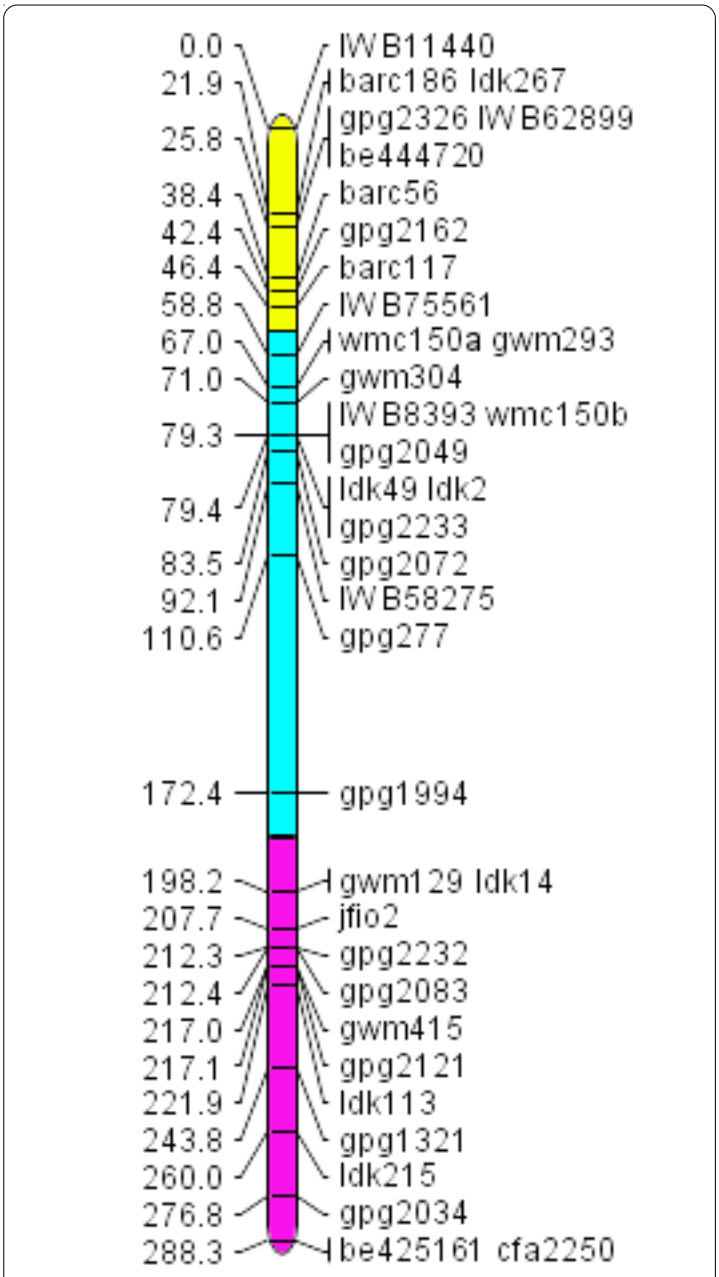

Figure 9 *Radiation hybrid map of 5A chromosome short arm based on 35 makers and 40 informative lines obtained from pollen irradiated CS-RH panel. Bin are presented in different colours, C-5AS1-0.40 in magenta, 5AS1-0.40-0.75 in cyan, and 5AS3-0.75-0.97 in yellow. Map distances are reported in cR (left). Marker order for the Del-NIL3 map is on the right side.*

3.3 Comparison of Del-NIL3 and CS-RH

Del-NIL3 panel consisting of 1764 plants and CS-RH composed of 276 RH_0 plants were screened for deletions. In the Del-NIL3 panel of 1764 analysed plants, 28 bear deletions on the short 5A arm (1.58%), while of 274 CS-RH lines, preliminary screening revealed 40 informative lines (14.59%).

Table 6 *Statistics summary of Del-NIL3, CS-RH, and consensus map derived from genotyping informative lines with 35 markers.*

	Del-NIL3	CS-RH	Consensus map
	mean (range)	mean (range)	mean (range)
No. of analysed lines	1764	276	2040
No. of markers	35	35	35
No. of informative lines	28	40	68
Map size (cR)	433.3	288.3	324.8
No. of double markers	17	21	6
No. of mapped loci	27	26	33
Markers per locus	1.29 (1 – 4)	1.34 (1 – 3)	1.06 (1 – 2)
Distance between two loci (cR)	16.04 (6.8 – 63.9)	11.08 (3.9 – 61.8)	9.84 (2.3 – 59.7)
Distance between two loci (Mbp)	10.58	10.96	8.66
No. of obligate breaks	49	58	107
No. of deletions	29	41	70
terminal	7	23	30
interstitial	22	18	40
Retention frequency per line	74.9 (0.00 – 97.22)	52.99 (5.56 – 97.22)	62.08 (0 – 97.22)
Retention frequency per marker	74.9 (64.29 – 92.86)	52.99 (32.5 – 97.5)	62.01 (50 – 95.59)
Deletion size (cR)	105.31 (13.20 – 433.3)	123.98 (10.3 – 282.55)	110.97 (4.85 – 324.8)
Deletion size (Mbp)	69.55 (8.72 – 286.15)	123.06 (10.22 – 280.44)	97.76 (4.27 – 286.15)
Resolution (Mbp/cR)	0.66	0.99	0.88

Following analysis with totally 35 markers (Table 6, Figure 10) realized maps covering 433.3 and 288.3 cR for Del-NIL3 and CS-RH with 27 and 26 mapped loci, respectively. Assuming even distribution of DSB, the distance between two loci in cR for Del-NIL3 is higher (16.04) than for CS-RH (11.08). However when converted to Mbp, the average distance between two loci is shorter in Del-NIL3 due to conversion factor (0.6 Mb/cR for Del-NIL3, 0.99 Mb/cR for CS-RH). With more informative lines it is expected to have higher number of obligate breaks, as observed in CS-RH panel. In seed irradiated panel 75% are interstitial deletions, compared to 44% in pollen irradiated. Retention frequency per line (Table 6, Figure 11) is higher in Del-NIL3 (74.9%) than in CS-RH (52.99%).

Average marker retention frequency for informative lines is higher in the pollen irradiation panel (47.01%) than in the seed irradiation panel (25.1%).

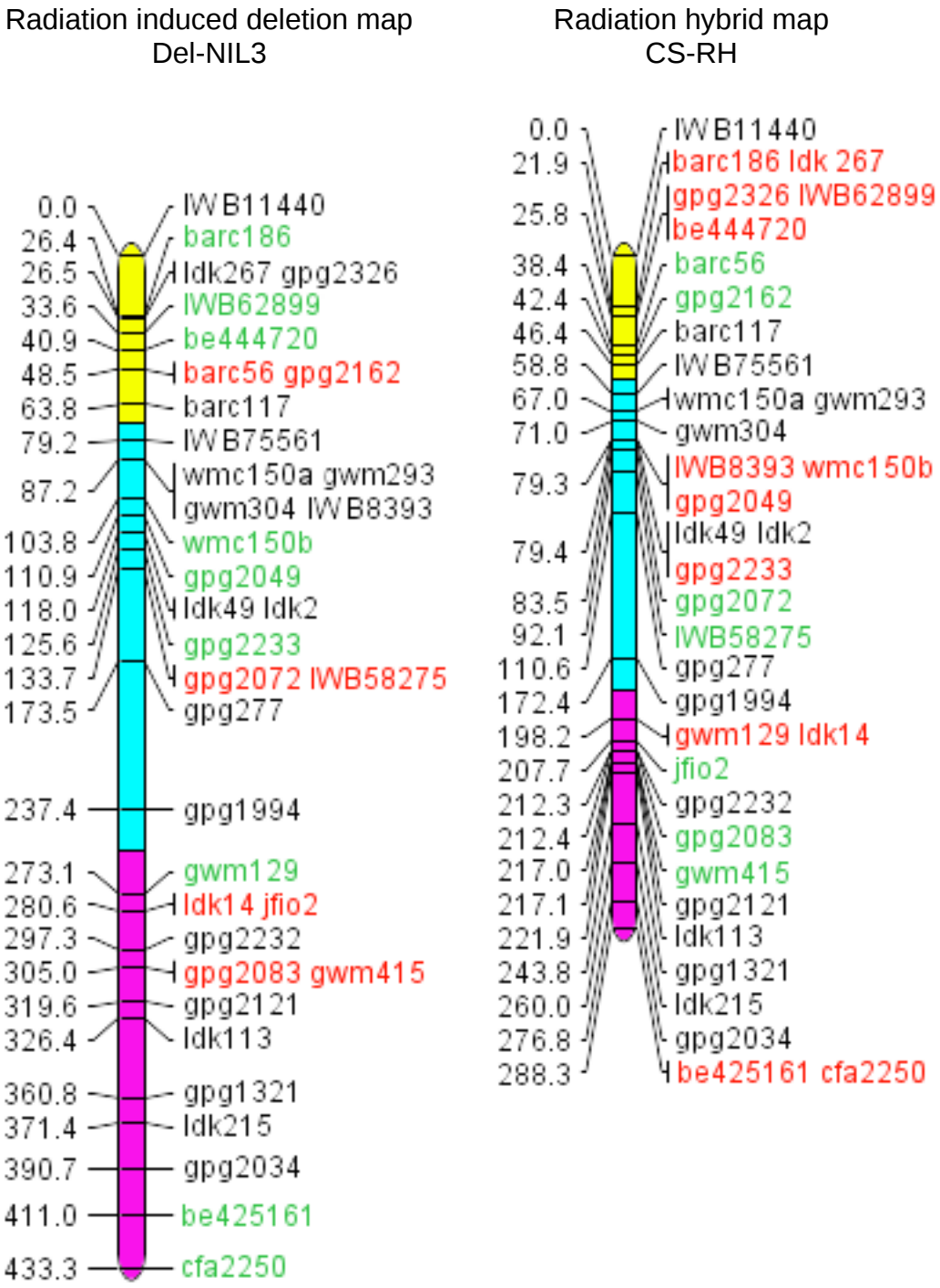

Figure 10 *Comparison of Del-NIL3 (left) and CS-RH (right) map. In both maps bins are coloured differently, C-5AS1-0.40 is coloured magenta, 5AS1-0.40-0.75 cyan, and 5AS3-0.75-0.97 yellow. Left from the chromosome are distances in cR, and on the right marker order for the given map. Red markers represents clusters of markers, and green markers are the same markers that were successfully separated in the other map.*

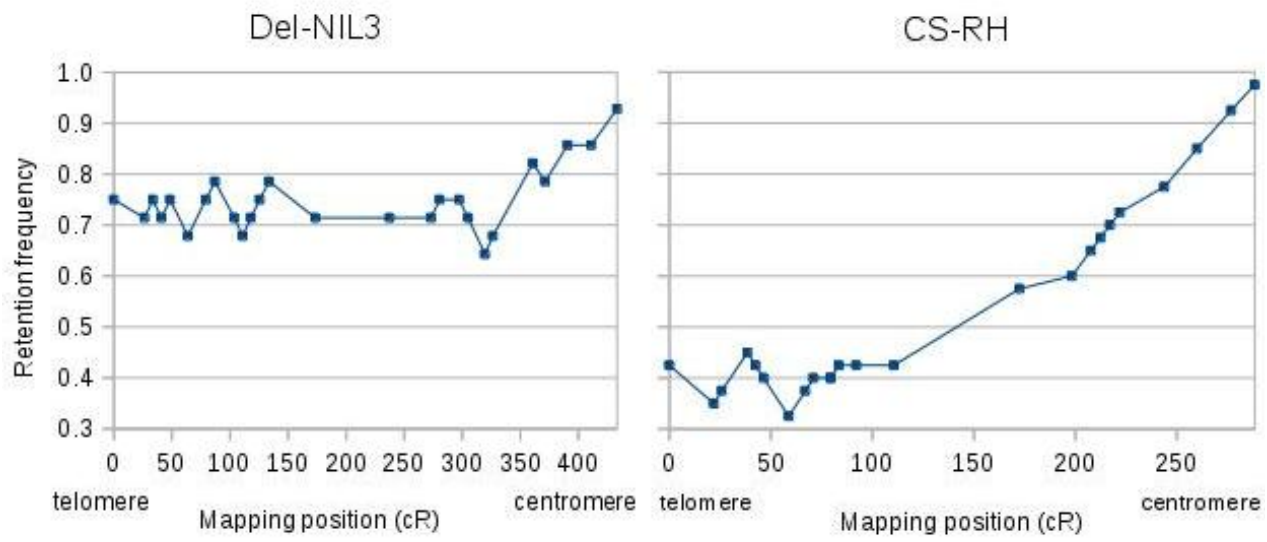

Figure 11 *Retention frequency at each locus for Del-NIL3 and CS-RH. Frequencies were calculated from 28 informative lines in the Del-NIL3 panel, and 40 in the CS-RH.*

In the Del-NIL3, according to the obtained marker data, two lines (D_393 and D_723) miss the whole short arm and are 433.3 cR in length (Figure 12), or 286.15 Mbp. The average deletion size is smaller in the Del-NIL3, with greater difference when Mbp sizes are compared, with CS-RH average sizes almost twofold bigger (123.06 Mbp) than Del-NIL3 (69.55).

Overall resolution (Mbp/cR) is higher in the Del-NIL3 (0.66) panel than in the CS-RH (0.99), due to the higher number of interstitial deletions.

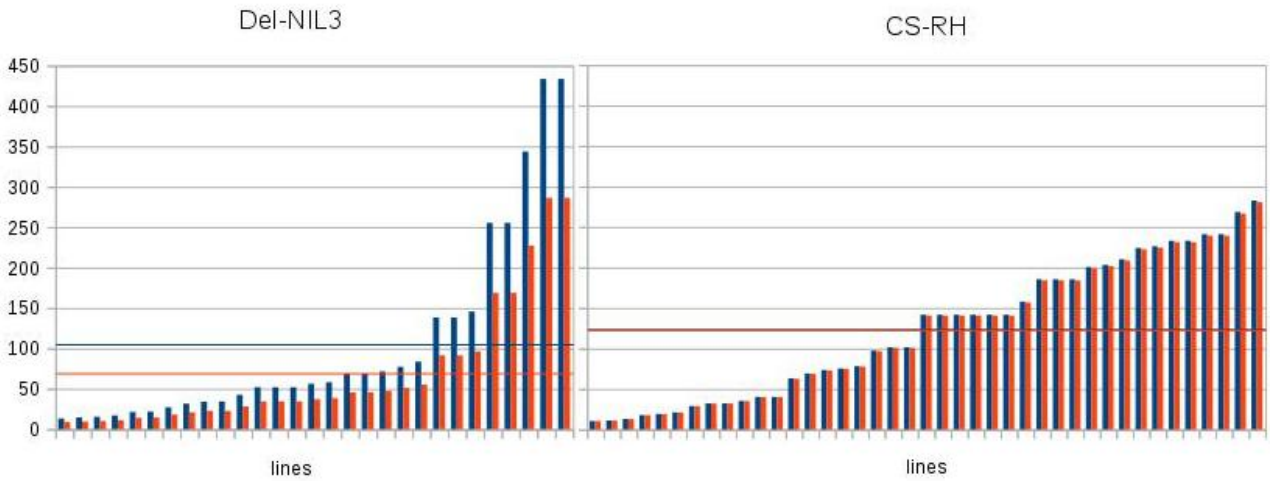

Figure 12 *Deletion sizes in cR and Mbp for Del-NIL and CS-RH. Blue columns represent sizes in cR, and red columns in Mbp. Blue line is an average deletion size in cR, and red line in Mbp.*

Counting obligate breaks for each bin implies an even distribution of breaks along the chromosome arm (Figure 13). In the all three maps, there is an interval with a higher number of obligate breaks. Interval *gpg277* – *gpg1994* counts 6, 10, and 16 for Del-NIL3, CS-RH, and the consensus map, respectively, indicating the greater distance between those two markers, and need for additional markers in that region.

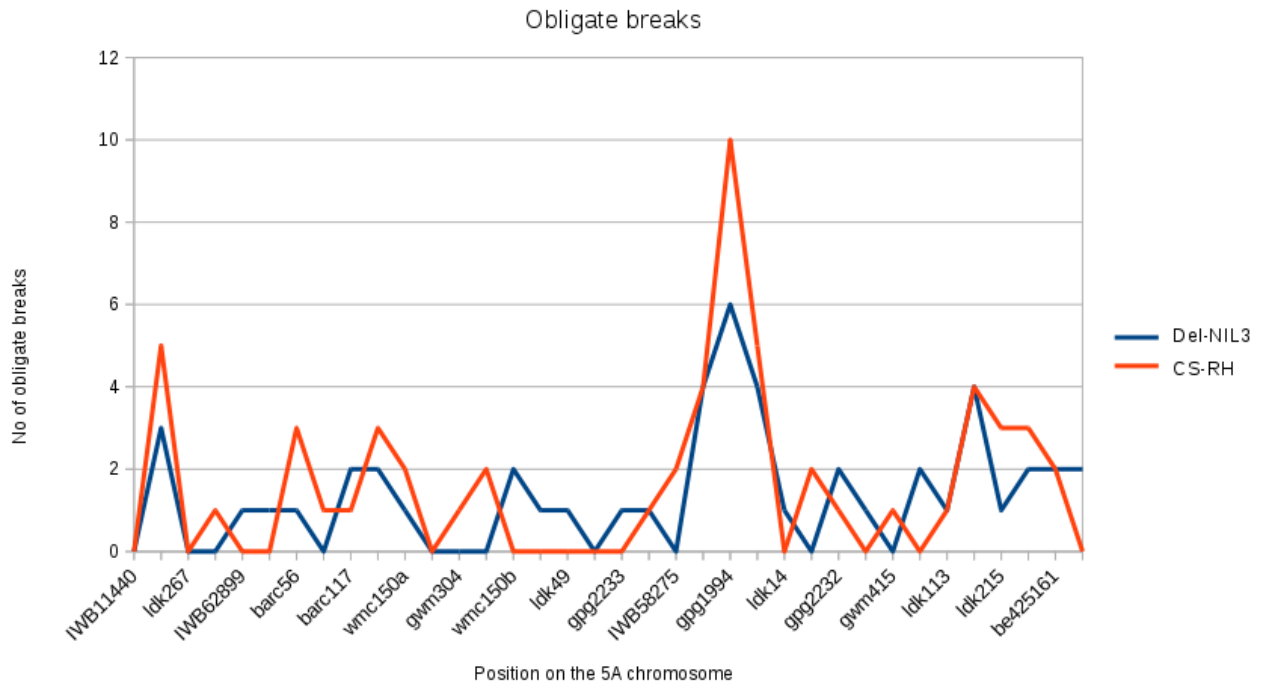

Figure 13 *Distribution of obligate breaks along the 5AS chromosome arm indicate the homogeneously induced deletions. Blue line represent obligate breaks induced in seed irradiated panel (Del-NIL3) and red line in pollen irradiated panel (CS-RH).*

3.4 Consensus Map

3.4.1 Characterization of the Informative Lines

Consensus map derived from 28 Del-NIL3 and 40 CS-RH informative lines (Table 7), resulted in marker retention frequency ranging from 50 to 95.59%, with the average value of 62.01%. Average marker retention frequency for C-5AS1-0.40, 5AS1-0.40-0.75, and 5AS3-0.75-0.97 was 76.02%, 54.83%, and 52.94%, respectively. Mean value for the retention frequency per line is 62.08% (ranging from 0 to 97.22%). One hundred and seven obligate breaks are evenly distributed across the short arm, with 44 allocated to C-5AS1-0.40, and 5AS1-0.40-0.75, respectively, and 19 in the most distal bin (5AS3-0.75-0.97). Sixteen obligate breaks are positioned in the *gpg277* and *gpg1994* interval.
The order of markers was generally consistent with previous publications. There were four cases (Xbarc186, gpg2326, Xgwm304, ldk14) of inconsistencies (Table 8).

3.4.2 Generating a Consensus Map

Consensus map, established on the 68 informative lines, covered the distance of 324.8 cR, and mapped 35 markers to 33 unique positions on the 5A short arm (Figure 14). The average distance between two loci was 9.84 cR, which corresponds to 8.66 Mbp. Calculated average deletion size is 110.97 cR or 97.76 Mbp. Overall resolution for the consensus map was 0.88 Mbp/cR.

3.4.3 Size of Deletions in the Consensus Map

To estimate the deletion sizes, acquired sizes in cR were multiplied by 0.88 conversion factor (Table 9). The average size of the deletion in the consensus map is 110.97 cR, which corresponds to 97.76 Mbp. Minimum deletion size was 4.85 in cR or 4.27 Mbp, while maximum deletion size was 324.8 cR or 286.15 Mbp. Average deletion size calculated for maximum retention frequency per line (97.22), ranged from 10.05 to 41.45 in cR, or 8.85 to 35.52 in Mbp.

Table 7 *Marker data for 68 informative lines in consensus map. Marker data shows overall marker arrangement and deletion positions for each line. On the left is given marker order on the 5AS, and their position in bins. Green fields (d) represent absent chromosome parts - deletions, yellow (1) present chromosome parts. Obligate breaks and retention frequency were calculated for each marker and per bin. Retention frequency per marker is presented by a colour scheme, red stands for lowest and green for the highest retention frequency. Distances between markers are given in cR and Mbp, and are accentuated with colours ranging from red (zero) to green (highest). Cumulative distance is given in cR. Resolution is a ratio of Mbp per cR and is calculated for each bin, and average.*

		Obligate breaks		Retention frequency		Distance between markers (cR)	Distance between markers (Mbp)	Cumulative distance (cR)	5AS = 295 Mbp/1C	Mb/cR
		per marker	per bin	per marker	per bin					
5AS3-0.75-0.97	IWB11440	0		55.88		0	0.00	0		
	barc186	8		50.00		21.6	28.90	21.6		
	ldk267	0		50.00		0	0.00	21.6		
	gpg2326	1		51.47		2.3	3.08	23.9		
	IWB62899	1	19	52.94	52.94	2.3	3.08	26.3	64.9	1.34
	be444720	1		51.47		3	4.01	29.3		
	barc56	4		57.35		9.5	12.71	38.7		
	gpg2162	1		55.88		2.4	3.21	41.1		
	barc117	3		51.47		7.4	9.90	48.5		
5AS1-0.40-0.75	IWB75561	5		50.00		12.6	9.77	61.2		
	wmc150a	3		54.41		7.5	5.82	68.6		
	gwm293	0		54.41		0	0.00	68.6		
	gwm304	1		55.88		2.5	1.94	71.1		
	IWB8393	2		55.88		5	3.88	76.1		
	wmc150b	2		52.94		5	3.88	81.1		
	gpg2049	1	44	51.47	54.83	2.4	1.86	83.5	103.25	0.78
	ldk49	1		52.94		2.4	1.86	85.9		
	ldk2	0		52.94		0	0.00	85.9		
	gpg2233	1		54.41		2.4	1.86	88.4		
	gpg2072	2		57.35		5.1	3.96	93.4		
	IWB58275	2		57.35		5.3	4.11	98.7		
	gpg277	8		54.41		23.2	18.00	121.9		
	gpg1994	16		63.24		59.7	46.31	181.6		
C-5AS1-0.40	gwm129	9		64.71		28.8	23.73	210.4		
	ldk14	1		66.18		2.7	2.22	213.1		
	jfio2	2		69.12		5.6	4.61	218.8		
	gpg2232	3		70.59		8.8	7.25	227.5		
	gpg2083	1		69.12		2.8	2.31	230.3		
	gwm415	1		70.59		2.8	2.31	233.1		
	gpg2121	2	44	67.65	76.02	5.7	4.70	238.8	118	0.82
	ldk113	2		70.59		5.7	4.70	244.5		
	gpg1321	8		79.41		26.3	21.67	270.9		
	ldk215	4		82.35		14.5	11.95	285.3		
	gpg2034	5		89.71		17.8	14.67	303.1		
	be425161	4		92.65		14.6	12.03	317.7		
	cfa2250	2		95.59		7	5.77	324.8		
		107		62.01			286.07		286.15	**0.88**

Table 8 *Position of molecular markers. Highlighted in red are discrepancies in marker order according to herein presented results and previous publications.*

Locus	Reference	5A bin according to literature	5A bin according to this study
Xbarc56-5A	(Somers et al., 2004)	5AS3-0.75-0.98	5AS3-0.75-0.97
Xbarc117-5A	(Somers et al., 2004)	5AS3-0.75-0.98	5AS3-0.75-0.97
Xbarc186-5A	(Somers et al., 2004)	C-5AL12-0.35 5AL17-0.78-0.87	5AS3-0.75-0.97
BE425161-5A	(Akhunov et al., 2010)	C-5AS1-0.40	C-5AS1-0.40
BE444720-5A	(Akhunov et al., 2010)	5AS3-0.75-0.98	5AS3-0.75-0.97
Xcfa2250-5A	(Sourdille et al., 2001) (Somers et al., 2004)	C-5AS1-0.40	C-5AS1-0.40
gpg277	(Barabaschi et al., 2015)	5AS1-0.40-0.75	5AS1-0.40-0.75
gpg1321	(Barabaschi et al., 2015)	C-5AS1-0.40	C-5AS1-0.40
gpg1994	(Barabaschi et al., 2015)	5AS1-0.40-0.75	5AS1-0.40-0.75
gpg2034	(Barabaschi et al., 2015)	C-5AS1-0.40	C-5AS1-0.40
gpg2049	(Barabaschi et al., 2015)	5AS1-0.40-0.75	5AS1-0.40-0.75
gpg2072	(Barabaschi et al., 2015)	5AS1-0.40-0.75	5AS1-0.40-0.75
gpg2083	(Barabaschi et al., 2015)	C-5AS1-0.40	C-5AS1-0.40
gpg2121	(Barabaschi et al., 2015)	C-5AS1-0.40	C-5AS1-0.40
gpg2162	(Barabaschi et al., 2015)	5AS3-0.75-0.97	5AS3-0.75-0.97
gpg2232	(Barabaschi et al., 2015)	C-5AS1-0.40	C-5AS1-0.40
gpg2233	(Barabaschi et al., 2015)	5AS1-0.40-0.75	5AS1-0.40-0.75
gpg2326	(Barabaschi et al., 2015)	C-5AS1-0.40	5AS3-0.75-0.97
Xgwm129-5A	(Röder et al., 1998)	C-5AS1-0.40	C-5AS1-0.40
Xgwm293-5A	(Röder et al., 1998) (Somers et al., 2004)	5AS1-0.40-0.75	5AS1-0.40-0.75
Xgwm304-5A	(Röder et al., 1998) (Somers et al., 2004)	C-5AS1-0.40	5AS1-0.40-0.75
Xgwm415-5A	(Röder et al., 1998) (Somers et al., 2004)	C-5AS1-0.40	C-5AS1-0.40
iwb8393	(Wang et al., 2014)	5AS1-0.40-0.75	5AS1-0.40-0.75
iwb11440	(Wang et al., 2014)	5AS3-0.75-0.97	5AS3-0.75-0.97
iwb58275	(Wang et al., 2014)	5AS1-0.40-0.75	5AS1-0.40-0.75
iwb62899	(Wang et al., 2014)	5AS3-0.75-0.97	5AS3-0.75-0.97
iwb75561	(Wang et al., 2014)	5AS1-0.40-0.75	5AS1-0.40-0.75
jfio2	(Barabaschi et al., 2015)	C-5AS1-0.40	C-5AS1-0.40
ldk2	(Barabaschi et al., 2015)	5AS1-0.40-0.75	5AS1-0.40-0.75
ldk14	(Barabaschi et al., 2015)	5AS1-0.40-0.75	C-5AS1-0.40
ldk49	(Barabaschi et al., 2015)	5AS1-0.40-0.75	5AS1-0.40-0.75
ldk113	(Barabaschi et al., 2015)	C-5AS1-0.40	C-5AS1-0.40
ldk215	(Barabaschi et al., 2015)	C-5AS1-0.40	C-5AS1-0.40
ldk267	(Barabaschi et al., 2015)	5AS3-0.75-0.97	5AS3-0.75-0.97
Xwmc150-5A	(Somers et al., 2003)	5AS1-0.40-0.75	5AS1-0.40-0.75

Table 9 *Population characterization and estimation of deletion sizes (in cR and Mbp) in consensus map*

Line	Retention frequency	Obligate breaks	Deletion size (cR)			Deletion size (Mbp)		
			Max	Min	Average	Max	Min	Average
D_393	**0.00**	0	324.8	324.8	**324.8**	286.15	286.15	**286.15**
D_723	**0.00**	0	324.8	324.8	324.8	286.15	286.15	286.15
CS_75	5.56	1	317.7	303.1	310.4	279.89	267.03	273.46
CS_30	8.33	1	303.1	285.3	294.2	267.03	251.35	259.19
CS_131	13.89	2	285.3	249.3	267.3	251.35	219.63	235.49
CS_141	13.89	2	285.3	249.3	267.3	251.35	219.63	235.49
CS_163	13.89	1	270.9	244.5	257.7	238.66	215.41	227.03
CS_2	13.89	1	270.9	244.5	257.7	238.66	215.41	227.03
D_291	13.89	1	270.9	244.5	257.7	238.66	215.41	227.03
CS_168	27.78	1	227.5	218.8	223.15	200.43	192.76	196.60
CS_93	27.78	2	264.4	244.2	254.3	232.94	215.14	224.04
CS_25	30.56	1	218.8	213.1	215.95	192.76	187.74	190.25
CS_54	30.56	2	262	236.8	249.4	230.82	208.62	219.72
CS_199	36.11	1	210.4	181.6	196	185.36	159.99	172.68
CS_32	36.11	1	210.4	181.6	196	185.36	159.99	172.68
CS_52	36.11	1	210.4	181.6	196	185.36	159.99	172.68
D_1077	36.11	1	210.4	181.6	196	185.36	159.99	172.68
D_1268	36.11	1	210.4	181.6	196	185.36	159.99	172.68
CS_117	38.89	1	181.6	121.9	151.75	159.99	107.39	133.69
CS_261	38.89	1	181.6	121.9	151.75	159.99	107.39	133.69
CS_27	38.89	1	181.6	121.9	151.75	159.99	107.39	133.69
CS_62	38.89	1	181.6	121.9	151.75	159.99	107.39	133.69
CS_67	38.89	1	181.6	121.9	151.75	159.99	107.39	133.69
CS_73	38.89	1	181.6	121.9	151.75	159.99	107.39	133.69
CS_120	41.67	1	121.9	98.7	110.3	107.39	86.96	97.17
CS_88	41.67	1	121.9	98.7	110.3	107.39	86.96	97.17
CS_156	50.00	2	199.8	168.4	184.1	176.02	148.36	162.19
CS_212	55.56	1	231.4	226.1	228.75	203.86	199.19	201.53
CS_247	63.89	1	76.1	71.1	73.6	67.04	62.64	64.84
CS_80	66.67	1	71.1	68.6	69.85	62.64	60.44	61.54
D_627	66.67	3	59.6	54.2	56.9	52.51	47.75	50.13
			21.6	0	10.8	19.03	0.00	9.51
CS_118	69.44	2	50.2	32.2	41.2	44.23	28.37	36.30
CS_134	69.44	2	136.1	92.7	114.4	119.90	81.67	100.79
D_1303	69.44	2	136.1	92.7	114.4	119.90	81.67	100.79
CS_122	72.22	2	44.9	27.2	36.05	39.56	23.96	31.76
CS_262	72.22	1	68.6	61.2	64.9	60.44	53.92	57.18
D_1537	75.00	1	61.2	48.5	54.85	53.92	42.73	48.32
D_175	75.00	2	149	62.9	105.95	131.27	55.42	93.34
D_451	75.00	2	149	62.9	105.95	131.27	55.42	93.34
CS_9	77.78	2	122.6	57.2	89.9	108.01	50.39	79.20
D_612	80.56	2	45.8	15.2	30.5	40.35	13.39	26.87
CS_112	83.33	4	20.1	0	10.05	17.71	0.00	8.85
			38.7	7.7	23.2	34.09	6.78	20.44
CS_218	83.33	2	14.3	2.8	8.55	12.60	2.47	7.53
CS_271	83.33	1	38.7	29.3	34	34.09	25.81	29.95
CS_4	83.33	1	38.7	29.3	34	34.09	25.81	29.95
D_1494	86.11	2	17.3	7.3	12.3	15.24	6.43	10.84
D_164	86.11	2	38.7	7.7	23.2	34.09	6.78	20.44
D_391	88.89	2	70	46.5	58.25	61.67	40.97	51.32
D_457	88.89	2	25.7	11.3	18.5	22.64	9.96	16.30
D_515	88.89	2	105.6	37.2	71.4	93.03	32.77	62.90
D_573	88.89	2	43.4	14.2	28.8	38.24	12.51	25.37
D_725	88.89	2	70	46.5	58.25	61.67	40.97	51.32
D_1433	91.67	2	7.3	2.4	**4.85**	6.43	2.11	**4.27**
D_1612	91.67	2	53.9	32.4	43.15	47.49	28.54	38.02
D_426	91.67	2	26.3	2.3	14.3	23.17	2.03	12.60
CS_186	94.44	2	37.2	2.7	19.95	32.77	2.38	17.58
CS_81	94.44	2	23.9	0	11.95	21.06	0.00	10.53
D_628	94.44	2	27.5	12.7	20.1	24.23	11.19	17.71
CS_140	**97.22**	2	40.8	0	20.4	35.94	0.00	17.97
CS_42	**97.22**	1	21.6	0	10.8	19.03	0.00	9.51
CS_94	**97.22**	2	82.9	0	41.45	73.04	0.00	36.52
CS_97	**97.22**	2	82.9	0	41.45	73.04	0.00	36.52
D_1075	**97.22**	2	82.9	0	41.45	73.04	0.00	36.52
D_1604	**97.22**	2	82.9	0	41.45	73.04	0.00	36.52
D_1988	**97.22**	2	82.9	0	41.45	73.04	0.00	36.52
D_473	**97.22**	2	20.1	0	10.05	17.71	0.00	8.85
D_479	**97.22**	2	31.5	0	15.75	27.75	0.00	13.88
D_752	**97.22**	2	21.7	0	10.85	19.12	0.00	9.56
	62.08	**107**	**126.89**	**95.05**	**110.97**	**111.79**	**83.74**	**97.76**

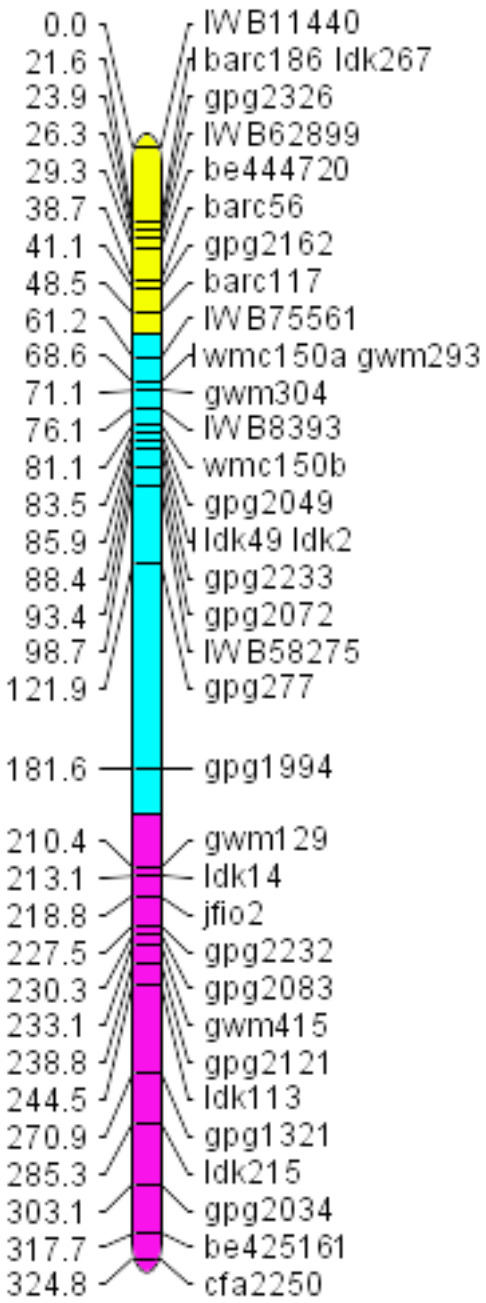

Figure 14 *Visual representation of 5AS consensus map based on 35 makers and 68 informative lines obtained from seed irradiate Del-NIL3 and pollen irradiated CS-RH panel. Bin are presented in different colours, C-5AS1-0.40 in magenta, 5AS1-0.40-0.75 in cyan, and 5AS3-0.75-0.97 in yellow. Map distances are reported in cR (left). Marker order for the Del-NIL3 map is on the right side.*

3.5 Comparison of the 5AS Chromosome Consensus Map with the NIL-RIL Genetic Map

Previous study conducted at the IFA genotyped 3650 NI-RILs with 13 polymorphic markers located on 5AS, and 3 on 5AL. Seventy-two NI-RILs showed a recombination in the *Qfhs.ifa-5A* support interval. All lines showing recombination between flanking markers *Xbarc186* and *Xbarc180* were further validated for FHB resistance in field test in two consecutive years (2014 and 2015). Analysed lines formed 16 haplotypes, and the genetic map covered a distance of 2.8 cM.

For the purpose of this study, resolution of the genetic map was calculated and compared to the consensus map, for the region between *barc186* and *cfa2250*. Focusing on that sole interval, the genetic map covered the distance of 1.2 cM, while the consensus map for the same section was 303.2 cR. Between the *barc186* and *cfa2250* only 13 markers were polymorphic, and thus could be used for genotyping, unlike 34 markers that were used for the same region in the consensus map. Thirteen polymophic markers were allocated to 6 loci in the NI-RIL genetic map (2.17 marker per locus), while 34 markers were assigned to 32 loci in the consensus map (1.06 marker per locus). The resolution of the genetic map was 238.46 Mbp/cM for the whole short arm (286.15 Mbp/1.2 cM). Consensus map provided a resolution of 0.94 Mbp/cR (286.15 Mbp/303.2 cR) (Figure 15).

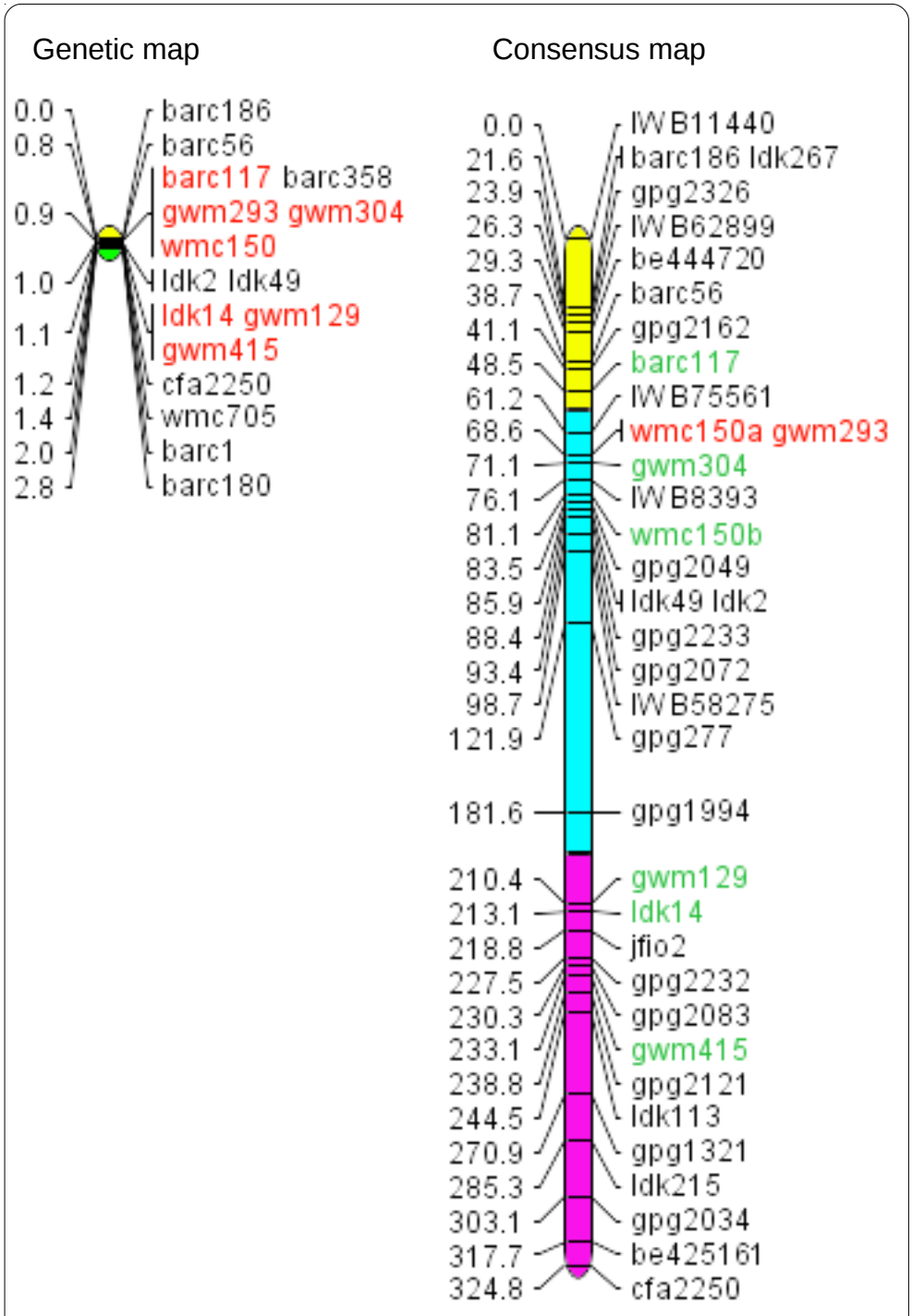

Figure 15 *Comparison of genetic (left) and consensus (right) map. Bins on the short arm are coloured differently, C-5AS1-0.40 is coloured magenta, 5AS1-0.40-0.75 cyan, and 5AS3-0.75-0.97 yellow. Long arm is coloured green. Left from the chromosome are distances in cR, and on the right marker order for the given map. Red markers represents clusters of markers, and green markers are the same markers that were successfully separated in the other map.*

4 DISCUSSION

A consensus map was derived from the Del-NIL3 and CS-RH maps. Del-NIL3 panel was created by irradiating seeds and propagating them by selfing to M_3. CS-RH population was developed by pollinating 'Chinese Spring' aneuploid line nulli-5A-tetra-5B with irradiated pollen of CS. Both panels were surveyed for the presence of deletions on the 5AS and selected for fine mapping. Seed irradiation resulted in fewer lines bearing a deletion (1.5%, 28 out of 1764), than pollen irradiation (14,5%, 40 out of 276 analysed plants), although seed irradiated panel was more than 6-fold bigger. This remarkable difference was previously reported by Tiwari et al. (2012). Possible explanation could be due to two different irradiation approaches. Pollen irradiation generates tissue harbouring more deletions than seed irradiation methods, because chromosomal breakage is induced after the final microgametophyte mitotic divisions (Tiwari et al., 2012). Seed irradiation might bear fewer detectable deletions due to (i) meiotic sieve. Meiosis fails to function properly in tissues with major chromosomal abnormalities (Richards, 1997) leading to production of non-viable seeds. Only (ii) homozygous deletion could be detected, which requires a selfing cycle. During selfing not all deletions are transferred to the next generation. Deletions are inherited according to Mendel segregation ratio, meaning that only one out of four plants would have deletions in homozygous state. This also results in smaller deletions, which are not simple to detect. Screening with higher number of markers might be helpful.

Both maps allocated approximately the same number of loci (Table 6). According to number of screened lines, it is evident that fewer plants need to be screened in CS-RH panel to obtain same number of loci. Pollen irradiation technique induced longer deletions. This is especially striking in physical distances (Mbp), due to the different resolution (Mbp/cR). Deletions induced in pollen were almost double in size (123.06 Mbp) than those derived from irradiated seeds (69.55 Mbp). Moreover, irradiated pollen carried more terminal deletions (56%), whereas irradiated seeds had more interstitial deletions (75%), which is in disagreement with previously published studies where pollen irradiation resulted in more interstitial deletions in *Arabidopsis* (Vizir and Mulligan, 1999) and wheat (Tiwari et al. 2012). Higher occurrence of interstitial deletions in Del-NIL3 sub-panel gives higher number of DSB leading to higher map resolution with fewer informative lines. The majority of terminal deletions in the CS-RH panel affects the distribution of retention

frequency for each marker. Due to the cumulative effect of the background terminal deletions, average marker loss per bin increases with increasing distance from the centromere.

4.1 Marker Retention Frequencies

Mainly deletions of smaller size were identified in the Del-NIL3, causing 1.4-fold greater retention frequency per marker opposed to CS-RH panel. Presumably, larger deletions that are more deleterious or lethal, were purged from the panel during the selfing step. Average retention frequency in Del-NIL3 corresponds to the previous publications (Hossain et al., 2004b, Gao et al., 2006, Kalavacharla, 2006, Tiwari et al., 2012), while CS-RH exhibits higher marker loss.

4.2 Mapping Resolution

Radiation hybrid map resolution is a function of the number of analysed lines, quantity of chromosome breaks dependent on the applied dosage, marker distribution, and retention patterns (Tiwari et al., 2016). Kumar et al. (2015) indicates the importance of large panels for RH mapping in plants. In general, RH panels in plants have lower deletion frequency than those in animals. For instance, RH map of the D genome of *Aegilops tauschii* showed 11.7% of marker deleted while in average 70 to 80% of the marker were deleted in RH panels of animals (Faraut et al., 2009). Additionally, studies have shown that more analysed lines provide fewer linkage groups, and produce more accurate map information. In this study, a total of 35 markers were mapped to 27, 26, and 33 loci in the Del-NIL3, CS-RH, and consensus map, respectively. Meaning that Del-NIL3 could resolve marker order of 77%, CS-RH 74%, and consensus 94% markers. This demonstrates the power of RH mapping in separating genetically linked markers. The precision of a RH map is defined by the resolution, expressed in the megabase pairs (Mbp) to centiRay (cR) ratio. The present maps display an average mapping resolution of 0.66 Mbp/cR, 0.992 Mbp/cR, and 0.88 Mbp/cR for Del-NIL3, CS-RH, and the consensus map, respectively. Interestingly, both Del-NIL3 and CS-RH have the highest mapping resolution in the interstitial 5AS1-0.40-0.75 bin, followed by the pericentromeric C-5AS1-0.40 bin, and the lowest resolution in the

telomeric bin 5AS3-0.75-0.9. Consensus map shows the highest resolution in the bin closest to the centromere and decreases with approaching the telomere, reaching a 3.7-fold higher mapping potential around the centromere. These results demonstrate the importance of larger panels as well as marker saturation for obtaining a high resolution map.

4.3 Comparison of the 5AS Chromosome Consensus Map with NIL-RIL Genetic Map

Genetic map based on genotypic information from NI-RIL was compared to consensus map derived from informative lines of seed and pollen irradiated panels, for the *barc186* to *cfa2250* interval stretching on the short arm of the 5A.

Marker order was consistent in both maps. Consensus map successfully resolved most of marker clusters. Potency of resolving clusters lies in evenly distributed chromosomal breakages caused by radiation. Induced deletions are independent on chromosomal structure and region (Riera-Lizarazu et al., 2000, Gao et al., 2006, Riera-Lizarazu et al., 2010). Ability to allocate non-polymorphic markers in radiation induced mapping approach (Hossain et al., 2004b; Wardrop et al., 2004; Kalavacharla, 2006) resulted in 2-fold increase in mapped markers. Calculated ratio of cR per cM, estimated a 253-fold improved map resolution. Such a drastic increase in map resolution was previously published in the 3H barley map for the pericentromeric region, >262,4-fold (Mazaheri et al., 2015).

Due to the repressed recombination in the pericentromeric region and necessity of polymorphic markers, the genetic map failed to provide a high resolution map for the *Qfhs.ifa-5A* supporting interval, despite the high number of analysed lines. On the other hand, radiation induced mapping approach was able to map more markers, resolve clusters, and provide uniform, high resolution map with fewer lines.

5 CONCLUSION AND OUTLOOK

Fusarium head blight is a sever disease in small grain cereals, controlled by several QTL. One important QTL, *Qfhs.ifa-5A* is located near the centromere on the 5A short arm. Recombination around the centromere is reduced, which affects the availability of high resolution genetic maps. Radiation hybrid is an alternative method based on radiation induced chromosomal breaks. Radiation creates breakages randomly and homogeneously along the chromosomes. Evenly distributed breaks and the possibility to use monomorphic markers lead to higher resolution in RH mapping.

In this study, two panels were screened for deletions and informative lines were further subjected to fine mapping. Del-NIL3 panel was created by irradiating seeds, and CS-RH by irradiating pollen. From the comparison of genetic and consensus RH map it is evident that radiation hybrid mapping is a more powerful method, it is especially efficient in mapping low recombination regions.

Future objective should be phenotyping Del-NIL3 informative lines. Deletion lines having the resistance gene(s) deleted are assumed to be more susceptible than the wild-type line, allowing to associate deleted DNA sequences with the FHB phenotype. Although these results present significant progress in providing detail map, there is still space for further improvement. Analysing more lines with more markers should yield in better resolution. Final aim is to more precisely locate *Qfhs.ifa-5A* and eventually identify the underlying gene(s). Radiation hybrid mapping, as a recombination independent approach, appears suitable for supporting positional cloning of *Qfhs.ifa-5A*.

6 REFERENCES

Akhunov, E.D., Goodyear, A.W., Geng, S., Qi, L.-L., Echalier, B., Gill, B.S., Gustafson, J.P., Lazo, G., Chao, S., Anderson, O.D., Linkiewicz, A.M., Dubcovsky, J., La Rota, M., Sorrels, M.E., Zhang, D., Nguyen, H.T., Kalavacharla, V., Hossain, K., Kianian, S.F., Peng, J., Lapitan, N.L.V., Gonzalez-Hernandez, J.L., Anderson, J.A., Choi, D-W., Close, T.J., Dilbirligi, M., Gill, K.S., Walker-Simmons, M.K., Steber, C., McGuire, P.E., Qualset, C.O., Dvorak, J., 2003. The organization and rate of evolution of wheat genomes are correlated with recombination rates along chromosome arms. Genome Research 13, 753–763.

Akhunov, E.D., Akhunova, A.R., Anderson, O.D., Anderson, J.A., Blake, N., Clegg, M.T., Coleman-Derr, D., Conley, E.J., Crossman, C.C., Deal, K.R., Dubcovsky, J., Gill, B.S., Gu, Y.Q., Hadam, J., Heo, H., Huo, N., Lazo, G.R., Luo, M.-C., Ma, Y.Q., Matthews, D.E., McGuire, P.E., Morrell, P.L., Qualset, C.O., Renfro, J., Tabanao, D., Talbert, L.E., Tian, C., Toleno, D.M., Warburton, M.L., You, F.M., Zhang, W., Dvorak, J., 2010. Nucleotide diversity maps reveal variation in diversity among wheat genomes and chromosomes. BMC genomics 11, 702. doi:10.1186/1471-2164-11-702

Bai, G., Kolb, F.L., Shaner, G., Domier, L.L., 1999. Amplified fragment length polymorphism markers linked to a major quantitative trait locus controlling scab resistance in wheat. Phytopathology 89, 343–348.

Ban, T., Watanabe, N., 2001. The effects of chromosomes 3A and 3B on resistance to Fusarium head blight in tetraploid wheat. Hereditas 135, 95–99.

Barabaschi, D., Magni, F., Volante, A., Gadaleta, A., Šimková, H., Scalabrin, S., Prazzoli, M.L., Bagnaresi, P., Lacrima, K., Michelotti, V., Desiderio, F., Orrù, L., Mazzamurro, V., Fricano, A., Mastrangelo, A., Tononi, P., Vitulo, N., Jurman, I., Frenkel, Z., Cattonaro, F., Morgante, M., Blanco, A., Doležel, J., Delledonne, M., Stanca, A.M., Cattivelli, L., Valè, G., 2015. Physical Mapping of Bread Wheat Chromosome 5A: An Integrated Approach. The Plant Genome 8, 1–80. doi:10.3835/plantgenome2015.03.0011

Bassi, F.M., Kumar, A., Zhang, Q., Paux, E., Huttner, E., Kilian, A., Dizon, R., Feuillet, C., Xu, S.S., Kianian, S.F., 2013. Radiation hybrid QTL mapping of *Tdes2* involved in the first meiotic division of wheat. Theoretical and Applied Genetics 126, 1977–1990. doi:10.1007/s00122-013-2111-z

Bernstein, K.A., Rothstein, R., 2009. At Loose Ends: Resecting a Double-Strand Break. Cell 137, 807–810. doi:10.1016/j.cell.2009.05.007

Bleuyard, J.-Y., Gallego, M.E., White, C.I., 2006. Recent advances in understanding of the DNA double-strand break repair machinery of plants. DNA Repair 5, 1–12. doi:10.1016/j.dnarep.2005.08.017

Britt, A.B., 1999. Molecular genetics of DNA repair in higher plants. Trends in Plant Science 4, 20–25. doi:10.1016/S1360-1385(98)01355-7

Buerstmayr, H., Lemmens, M., Hartl, L., Doldi, L., Steiner, B., Stierschneider, M., Ruckenbauer, P., 2002. Molecular mapping of QTLs for Fusarium head blight resistance in spring wheat. I. Resistance to fungal spread (Type II resistance). Theoretical and Applied Genetics 104, 84–91.

Buerstmayr, H., Steiner, B., Hartl, L., Griesser, M., Angerer, N., Lengauer, D., Miedaner, T.,

Schneider, B., Lemmens, M., 2003. Molecular mapping of QTLs for Fusarium head blight resistance in spring wheat. II. Resistance to fungal penetration and spread. Theoretical and Applied Genetics 107, 503–508. doi:10.1007/s00122-003-1272-6

Buerstmayr, H., Ban, T., Anderson, J., 2009. QTL mapping and marker-assisted selection for Fusarium head blight resistance in wheat: a review. Plant Breeding 128, 1–26.

Chapman, J.A., Mascher, M., Buluç, A., Barry, K., Georganas, E., Session, A., Strnadova, V., Jenkins, J., Sehgal, S., Oliker, L., Schmutz, J., Yelick, K.A., Scholz, U., Waugh, R., Poland, J.A., Muehlbauer, G.J., Stein, N., Rokhsar, D.S., 2015. A whole-genome shotgun approach for assembling and anchoring the hexaploid bread wheat genome. Genome Biology 16. doi:10.1186/s13059-015-0582-8

Choulet, F., Alberti, A., Theil, S., Glover, N., Barbe, V., Daron, J., Pingault, L., Sourdille, P., Couloux, A., Paux, E., Leroy, P., Mangenot, S., Guilhot, N., Gouis, J.L., Balfourier, F., Alaux, M., Jamilloux, V., Poulain, J., Durand, C., Bellec, A., Gaspin, C., Safar, J., Dolezel, J., Rogers, J., Vandepoele, K., Aury, J.-M., Mayer, K., Berges, H., Quesneville, H., Wincker, P., Feuillet, C., 2014. Structural and functional partitioning of bread wheat chromosome 3B. Science 345, 1249721. doi:10.1126/science.1249721

Conley, E.J., Nduati, V., Gonzalez-Hernandez, J.L., Mesfin, A., Trudeau-Spanjers, M., Chao, S., Lazo, G.R., Hummel, D.D., Anderson, O.D., Qi, L.L., Gill, B.S., Echalier, B., Linkiewicz, A.M., Dubcovsky, J., Akhunov, E.D., Dvorak, J., Peng, J.H., Lapitan, N.L.V., Pathan, M.S., Nguyen, H.T., Ma, X.-F., Miftahudin, Gustafson, J.P., Greene, R.A., Sorrells, M.E., Hossain, K.G., Kalavacharla, V., Kianian, S.F., Sidhu, D., Dilbirligi, M., Gill, K.S., Choi, D.-W., Fenton, R.D., Close, T.J., McGuire, P.E., Qualset, C.O., Anderson, J.A., 2004. A 2600-Locus Chromosome Bin Map of Wheat Homoeologous Group 2 Reveals Interstitial Gene-Rich Islands and Colinearity With Rice. Genetics 168, 625–637. doi:10.1534/genetics.104.034801

de Bona, C.M., Stelly, D., Junior, J.C.M., Louzada, E.S., 2009. Fusion of protoplasts with irradiated microprotoplasts as a tool for radiation hybrid panel in citrus. Pesquisa Agropecuária Brasileira 44, 1616–1623.

de Givry, S., Bouchez, M., Chabrier, P., Milan, D., Schiex, T., 2005. CARTHAGENE: Multipopulation integrated genetic and radiation hybrid mapping. Bioinformatics 21, 1703–1704. doi:10.1093/bioinformatics/bti222

de Pontbriand, A., Wang, X.-P., Cavaloc, Y., Mattei, M.-G., Galibert, F., 2002. Synteny Comparison between Apes and Human Using Fine-Mapping of the Genome. Genomics 80, 395–401. doi:10.1006/geno.2002.6847

Don, R.H., Cox, P.T., Wainwright, B.J., Baker, K., Mattick, J.S., 1991. “Touchdown” PCR to circumvent spurious priming during gene amplification. Nucleic acids research 19, 4008. doi:10.1093/nar/19.14.4008

Endo, T.R., 1990. Gametocidal chromosomes and their induction of chromosome mutations in wheat. The Japanese Journal of Genetics 65, 135–152. doi:10.1266/jjg.65.135

Endo, T.R., 1988. Induction of chromosomal structural changes by a chromosome of *Aegilops cylindrica* L. in common wheat. Journal of Heredity 79, 366–370.

Endo, T.R., Gill, B.S., 1996. The deletion stocks of common wheat. Journal of Heredity 87, 295–307.

Faraut, T., de Givry, S., Hitte, C., Lahbib-Mansais, Y., Morisson, M., Milan, D., Schiex, T., Servin, B., Vignal, A., Galibert, F., Yerle, M., 2009. Contribution of Radiation Hybrids to Genome Mapping in Domestic Animals. Cytogenetic and Genome Research 126, 21–33. doi:10.1159/000245904

Feuillet, C., Leach, J.E., Rogers, J., Schnable, P.S., Eversole, K., 2011. Crop genome sequencing: lessons and rationales. Trends in Plant Science 16, 77–88. doi:10.1016/j.tplants.2010.10.005

Gadaleta, A., Giancaspro, A., Giove, S.L., Zacheo, S., Incerti, O., Simeone, R., Colasuonno, P., Nigro, D., Valè, G., Cattivelli, L., Stanca, M., Blanco, A., Donini, P., 2012. Development of a deletion and genetic linkage map for the 5A and 5B chromosomes of wheat (*Triticum aestivum*). Genome 55, 417–427. doi:10.1139/g2012-028

Gallagher, S.R., Desjardins, P.R., 2007. Quantitation of DNA and RNA with absorption and fluorescence spectroscopy. Current Protocols in Human Genetics A-3D. doi:10.1002/0471142301.nsa01ks56

Gao, W., Chen, Z.J., Yu, J.Z., Raska, D., Kohel, R.J., Womack, J.E., Stelly, D.M., 2004. Wide-Cross Whole-Genome Radiation Hybrid Mapping of Cotton (*Gossypium hirsutum* L.). Genetics 167, 1317–1329. doi:10.1534/genetics.103.020479

Gao, W., Chen, Z.J., Yu, J.Z., Kohel, R.J., Womack, J.E., Stelly, D.M., 2006. Wide-cross whole-genome radiation hybrid mapping of the cotton (*Gossypium barbadense* L.) genome. Molecular Genetics and Genomics 275, 105–113. doi:10.1007/s00438-005-0069-5

Gautier, M., Eggen, A., 2004. The construction and use of radiation hybrid maps in genomic research, in: Encyclopedia of Genetics, Genomics, Proteomics and Bioinformatics. John Wiley & Sons, Ltd.

Gill, K.S., Gill, B.S., Endo, T.R., 1993. A chromosome region-specific mapping strategy reveals gene-rich telomeric ends in wheat. Chromosoma 102, 374–381.

Goss, S.J., Harris, H., 1975. New method for mapping genes in human chromosomes.

Griffiths, A.J., Miller, J.H., Suzuki, D.T., Lewontin, R.C., Gelbart, W.M., 2000. Deletions, in: An Introduction to Genetic Analysis. 7th Edition.

Gupta, P.K., 2008. Single-molecule DNA sequencing technologies for future genomics research. Trends in Biotechnology 26, 602–611. doi:10.1016/j.tibtech.2008.07.003

Henegariu, O., Heerema, N.A., Dloughy, S.R., Vance, G.H., Vogt, P.H., 1997. Multiplex PCR: critical parameters and step-by-step protocol. Biotechniques 23, 504–511. doi:10.1007/BF00928712

Hitte, C., Madeoy, J., Kirkness, E.F., Priat, C., Lorentzen, T.D., Senger, F., Thomas, D., Derrien, T., Ramirez, C., Scott, C., Evanno, G., Pullar, B., Cadieu, E., Oza, V., Lourgant, K., Jaffe, D.B., Tacher, S., Dréano, S., Berkova, N., André, C., Deloukas, P., Fraser, C., Lindblad-Toh, K., Ostrander, E.A., Galibert, F., 2005. Facilitating genome navigation: survey sequencing and dense radiation-hybrid gene mapping. Nat Rev Genet 6, 643–648. doi:10.1038/nrg1658

Hossain, K.G., Kalavacharla, V., Lazo, G.R., Hegstad, J., Wentz, M.J., Kianian, P.M.A., Simons, K., Gehlhar, S., Rust, J.L., Syamala, R.R., Obeori, K., Bhamidimarri, S., Karunadharma, P., Chao, S., Anderson, O.D., Qi, L.L., Echalier, B., Gill, B.S., Linkiewicz, A.M., Ratnasiri, A., Dubcovsky, J., Akhunov, E.D., Dvorak, J., Miftahudin, Ross, K., Gustafson, J.P., Radhawa, H.S., Dilbirligi, M., Gill, K.S., Peng, J.H., Lapitan, N.L.V., Greene, R.A., Bermudez-Kandianis, C.E., Sorrells, M.E., Feril, O., Pathan, M.S., Nguyen, H.T., Gonzalez-Hernandez, J.L., Conley, E.J., Anderson, J.A., Choi, D.-W., Fenton, R.D., Close, T.J., McGuire, P.E., Qualset, C.O., Kianian, S.F., 2004a. A Chromosome Bin Map of 2148 Expressed Sequence Tag Loci of Wheat Homoeologous Group 7. Genetics 168, 687–699. doi:10.1534/genetics.104.034850

Hossain, K.G., Riera-Lizarazu, O., Kalavacharla, V., Vales, M.I., Maan, S.S., Kianian, S.F.,

2004b. Radiation Hybrid Mapping of the Species Cytoplasm-Specific (*scs*^{ae}) Gene in Wheat. Genetics 168, 415–423. doi:10.1534/genetics.103.022590

Jones, H.B., 1996. Hybrid selection as a method of increasing mapping power for radiation hybrids. Genome research 6, 761–769.

Kalavacharla, V., 2006. High-Resolution Radiation Hybrid Map of Wheat Chromosome 1D. Genetics 173, 1089–1099. doi:10.1534/genetics.106.056481

Kalavacharla, V., Hossain, K., Riera-Lizarazu, O., Gu, Y., Maan, S.S., Kianian, S.F., 2009. Chapter 6 Radiation Hybrid Mapping in Crop Plants, in: Advances in Agronomy. Elsevier, pp. 201–222.

Koornneef, M., Veen, J.H. van der, 1980. Induction and analysis of gibberellin sensitive mutants in *Arabidopsis thaliana* (L.) heynh. Theoretical and Applied Genetics 58, 257–263. doi:10.1007/BF00265176

Koornneef, M., Dellaert, L.W.M., van der Veen, J.H., 1982. EMS- and radiation-induced mutation frequencies at individual loci in *Arabidopsis thaliana* (L.) Heynh. Mutation Research/Fundamental and Molecular Mechanisms of Mutagenesis 93, 109–123. doi:10.1016/0027-5107(82)90129-4

Koornneef, M., Hanhart, C.J., van der Veen, J.H., 1991. A genetic and physiological analysis of late flowering mutants in *Arabidopsis thaliana*. Molecular and General Genetics MGG 229, 57–66. doi:10.1007/BF00264213

Kumar, N., Kulwal, P.L., Balyan, H.S., Gupta, P.K., 2007. QTL mapping for yield and yield contributing traits in two mapping populations of bread wheat. Molecular Breeding 19, 163–177. doi:10.1007/s11032-006-9056-8

Kumar, A., Bassi, F.M., Paux, E., Al-Azzam, O., de Jimenez, M.M., Denton, A.M., Gu, Y.Q., Huttner, E., Kilian, A., Kumar, S., Goyal, A., Iqbal, M.J., Tiwari, V.K., Dogramaci, M., Balyan, H.S., Dhaliwal, H.S., Gupta, P.K., Randhawa, G.S., Feuillet, C., Pawlowski, W.P., Kianian, S.F., 2012a. DNA repair and crossing over favor similar chromosome regions as discovered in radiation hybrid of Triticum. BMC Genomics 13, 339. doi:10.1186/1471-2164-13-339

Kumar, A., Simons, K., Iqbal, M.J., de Jiménez, M.M., Bassi, F.M., Ghavami, F., Al-Azzam, O., Drader, T., Wang, Y., Luo, M.-C., Gu, Y.Q., Denton, A., Lazo, G.R., Xu, S.S., Dvorak, J., Kianian, P.M., Kianian, S.F., 2012b. Physical mapping resources for large plant genomes: radiation hybrids for wheat D-genome progenitor *Aegilops tauschii*. BMC Genomics 13, 597. doi:10.1186/1471-2164-13-597

Kumar, A., Bassi, F.M., Michalak de Jimenez, M.K., Ghavami, F., Mazaheri, M., Simons, K., Iqbal, M.J., Mergoum, M., Kianian, S.F., Kianian, P.M.A., 2014. Radiation Hybrids: A valuable Tool for Genetic, Genomic and Functional Analysis of Plant Genomes, in: Tuberosa, R., Graner, A., Frison, E. (Eds.), Genomics of Plant Genetic Resources. Springer Netherlands, Dordrecht, pp. 285–318.

Kumar, A., Seetan, R., Mergoum, M., Tiwari, V.K., Iqbal, M.J., Wang, Y., Al-Azzam, O., Šimková, H., Luo, M.-C., Dvorak, J., Gu, Y.Q., Denton, A., Kilian, A., Lazo, G.R., Kianian, S.F., 2015. Radiation hybrid maps of the D-genome of *Aegilops tauschii* and their application in sequence assembly of large and complex plant genomes. BMC Genomics 16. doi:10.1186/s12864-015-2030-2

Künzel, G., Korzun, L., Meister, A., 2000. Cytologically integrated physical restriction fragment length polymorphism maps for the barley genome based on translocation breakpoints. Genetics 154, 397–412.

Lin, F., Xue, S.L., Zhang, Z.Z., Zhang, C.Q., Kong, Z.X., Yao, G.Q., Tian, D.G., Zhu, H.L., Li, C.J., Cao, Y., Wei, J.B., Luo, Q.Y., Ma, Z.Q., 2006. Mapping QTL associated with

resistance to Fusarium head blight in the Nanda2419 x Wangshuibai population. II: Type I resistance. Theoretical and Applied Genetics 112, 528–535. doi:10.1007/s00122-005-0156-3

Lin, S., Kernighan, B.W., 1973. An Effective Heuristic Algorithm for the Traveling-Salesman Problem. Operations Research 21, 498–516.

Linkiewicz, A.M., Qi, L.L., Gill, B.S., Ratnasiri, A., Echalier, B., Chao, S., Lazo, G.R., Hummel, D.D., Anderson, O.D., Akhunov, E.D., Dvorak, J., Pathan, M.S., Nguyen, H.T., Peng, J.H., Lapitan, N.L.V., Miftahudin, Gustafson, J.P., La Rota, C.M., Sorrells, M.E., Hossain, K.G., Kalavacharla, V., Kianian, S.F., Sandhu, D., Bondareva, S.N., Gill, K.S., Conley, E.J., Anderson, J.A., Fenton, R.D., Close, T.J., McGuire, P.E., Qualset, C.O., Dubcovsky, J., 2004. A 2500-Locus Bin Map of Wheat Homoeologous Group 5 Provides Insights on Gene Distribution and Colinearity With Rice. Genetics 168, 665–676. doi:10.1534/genetics.104.034835

Liu, S., Pumphrey, M., Gill, B., Trick, H., Zhang, J., Doležel, J., Chalhoub, B., Anderson, J., 2008. Toward positional cloning of Fhb1, a major QTL for Fusarium head blight resistance in wheat. Cereal Research Communications 36, 195–201. doi:10.1556/CRC.36.2008.Suppl.B.15

Lukaszewski, A.J., Curtis, C.A., 1993. Physical distribution of recombination in B-genome chromosomes of tetraploid wheat. Theoretical and Applied Genetics 86, 121–127.

Luo, M.C., Deal, K.R., Akhunov, E.D., Akhunova, A.R., Anderson, O.D., Anderson, J.A., Blake, N., Clegg, M.T., Coleman-Derr, D., Conley, E.J., Crossman, C.C., Dubcovsky, J., Gill, B.S., Gu, Y.Q., Hadam, J., Heo, H.Y., Huo, N., Lazo, G., Ma, Y., Matthews, D.E., McGuire, P.E., Morrell, P.L., Qualset, C.O., Renfro, J., Tabanao, D., Talbert, L.E., Tian, C., Toleno, D.M., Warburton, M.L., You, F.M., Zhang, W., Dvorak, J., 2009. Genome comparisons reveal a dominant mechanism of chromosome number reduction in grasses and accelerated genome evolution in Triticeae. Proceedings of the National Academy of Sciences 106, 15780–15785.

Mazaheri, M., Kianian, P., Kumar, A., Mergoum, M., Seetan, R., Soltani, A., Lund, L.I., Pirseyedi, S.M., Denton, A.M., Kianian, S.F., 2015. Radiation Hybrid Map of Barley Chromosome 3H. The Plant Genome 8, 0. doi:10.3835/plantgenome2015.02.0005

Mesterhazy, A., Bartok, T., Mirocha, C.G., Komoroczy, R., 1999. Nature of wheat resistance to Fusarium head blight and the role of deoxynivalenol for breeding. Plant Breeding 118, 97–110. doi:10.1046/j.1439-0523.1999.118002097.x

Metzker, M.L., 2010. Sequencing technologies — the next generation. Nat Rev Genet 11, 31–46. doi:10.1038/nrg2626

Michalak de Jimenez, M.K., Bassi, F.M., Ghavami, F., Simons, K., Dizon, R., Seetan, R.I., Alnemer, L.M., Denton, A.M., Doğramacı, M., Šimková, H., Doležel, J., Seth, K., Luo, M.-C., Dvorak, J., Gu, Y.Q., Kianian, S.F., 2013. A radiation hybrid map of chromosome 1D reveals synteny conservation at a wheat speciation locus. Functional & Integrative Genomics 13, 19–32. doi:10.1007/s10142-013-0318-3

Miftahudin, M., Ross, K., Ma, X.-F., Mahmoud, A.A., Layton, J., Rodriguez Milla, M.A., Chikmawati, T., Ramalingam, J., Feril, O., Pathan, M.S., Surlan Momirovic, G., Kim, S., Chema, K., Fang, P., Haule, L., Struxness, H., Birkes, J., Yaghoubian, C., Skinner, R., McAllister, J., Nguyen, V., Qi, L.L., Echalier, B., Gill, B.S., Linkiewicz, A.M., Dubcovsky, J., Akhunov, E.D., Dvorak, J., Dilbirligi, M., Gill, K.S., Peng, J.H., Lapitan, N.L.V., Bermudez-Kandianis, C.E., Sorrells, M.E., Hossain, K.G., Kalavacharla, V., Kianian, S.F., Lazo, G.R., Chao, S., Anderson, O.D., Gonzalez-Hernandez, J., Conley, E.J., Anderson, J.A., Choi, D.-W., Fenton, R.D., Close, T.J., McGuire, P.E., Qualset, C.O., Nguyen, H.T., Gustafson, J.P., 2004. Analysis of Expressed Sequence Tag Loci on

Wheat Chromosome Group 4. Genetics 168, 651–663. doi:10.1534/genetics.104.034827

Munkvold, J.D., Greene, R.A., Bermudez-Kandianis, C.E., La Rota, C.M., Edwards, H., Sorrells, S.F., Dake, T., Benscher, D., Kantety, R., Linkiewicz, A.M., Dubcovsky, J., Akhunov, E.D., Dvorak, J., Miftahudin, Gustafson, J.P., Pathan, M.S., Nguyen, H.T., Matthews, D.E., Chao, S., Lazo, G.R., Hummel, D.D., Anderson, O.D., Anderson, J.A., Gonzalez-Hernandez, J.L., Peng, J.H., Lapitan, N., Qi, L.L., Echalier, B., Gill, B.S., Hossain, K.G., Kalavacharla, V., Kianian, S.F., Sandhu, D., Erayman, M., Gill, K.S., McGuire, P.E., Qualset, C.O., Sorrells, M.E., 2004. Group 3 Chromosome Bin Maps of Wheat and Their Relationship to Rice Chromosome 1. Genetics 168, 639–650. doi:10.1534/genetics.104.034819

Murphy, W.J., Larkin, D.M., Everts-van der Wind, A., Bourques, G., Tesler, G., Auvil, L., Beever, J.E., Chowdhary, B.P., Galibert, F., Gatzke, L., Hitte, C., Meyers, S.N., Milan, D., Ostrander, E.A., Pape, G., Parker, H.G., Raudsepp, T., Rogatscheva, M.B., Schook, L.B., Skow, L.C., Welge, M., Womack, J.E., O'Brien, S.J., Pevzner, P.A., Lewin, H.A., 2005. Dynamics of Mammalian Chromosome Evolution Inferred from Multispecies Comparative Maps. Science 309, 613–617. doi:10.1126/science.1111387

O'Brien, S.J., Menotti-Raymond, M., Murphy, W.J., Nash, W.G., Wienberg, J., Stanyon, R., Copeland, N.G., Jenkins, N.A., Womack, J.E., Graves, J.A.M., 1999. The promise of comparative genomics in mammals. Science 286, 458–481.

Oetting, W.S., Lee, H.K., Flanders, D.J., Wiesner, G.L., Sellers, T. a, King, R. a, 1995. Linkage analysis with multiplexed short tandem repeat polymorphisms using infrared fluorescence and M13 tailed primers. Genomics. doi:10.1006/geno.1995.1264

Paux, E., Sourdille, P., Salse, J., Saintenac, C., Choulet, F., Leroy, P., Korol, A., Michalak, M., Kianian, S., Spielmeyer, W., Lagudah, E., Somers, D., Kilian, A., Alaux, M., Vautrin, S., Berges, H., Eversole, K., Appels, R., Safar, J., Simkova, H., Dolezel, J., Bernard, M., Feuillet, C., 2008. A Physical Map of the 1-Gigabase Bread Wheat Chromosome 3B. Science 322, 101–104. doi:10.1126/science.1161847

Peng, J.H., Zadeh, H., Lazo, G.R., Gustafson, J.P., Chao, S., Anderson, O.D., Qi, L.L., Echalier, B., Gill, B.S., Dilbirligi, M., Sandhu, D., Gill, K.S., Greene, R.A., Sorrells, M.E., Akhunov, E.D., Dvorak, J., Linkiewicz, A.M., Dubcovsky, J., Hossain, K.G., Kalavacharla, V., Kianian, S.F., Mahmoud, A.A., Miftahudin, Conley, E.J., Anderson, J.A., Pathan, M.S., Nguyen, H.T., McGuire, P.E., Qualset, C.O., Lapitan, N.L.V., 2004. Chromosome Bin Map of Expressed Sequence Tags in Homoeologous Group 1 of Hexaploid Wheat and Homoeology With Rice and Arabidopsis. Genetics 168, 609–623. doi:10.1534/genetics.104.034793

Puchta, H., 2005. The repair of double-strand breaks in plants: mechanisms and consequences for genome evolution. Journal of Experimental Botany 56, 1–14. doi:10.1093/jxb/eri025

Qi, L., Echalier, B., Friebe, B., Gill, B.S., 2003. Molecular characterization of a set of wheat deletion stocks for use in chromosome bin mapping of ESTs. Functional & integrative genomics 3, 39–55.

Qi, L.L., Echalier, B., Chao, S., Lazo, G.R., Butler, G.E., Anderson, O.D., Akhunov, E.D., Dvorak, J., Linkiewicz, A.M., Ratnasiri, A., Dubcovsky, J., Bermudez-Kandianis, C.E., Greene, R.A., Kantety, R., La Rota, C.M., Munkvold, J.D., Sorrells, S.F., Sorrells, M.E., Dilbirligi, M., Sidhu, D., Erayman, M., Randhawa, H.S., Sandhu, D., Bondareva, S.N., Gill, K.S., Mahmoud, A.A., Ma, X.-F., Miftahundin, Gustafson, J.P., Conley, E.J., Nduati, V., Gonzalez-Hernandez, J.L., Anderson, J.A., Peng, J.H., Lapitan, N.L.V., Hossain, K.G., Kalavacharla, V., Kianian, S.F., Pathan, M.S., Zhang, D.S., Nguyen, H.T., Choi,

D.-W., Fenton, R.D., Close, T.J., McGuire, P.E., Qualset, C.O., Gill, B.S., 2004. A Chromosome Bin Map of 16,000 Expressed Sequence Tag Loci and Distribution of Genes Among the Three Genomes of Polyploid Wheat. Genetics 168, 701–712. doi:10.1534/genetics.104.034868

Randhawa, H.S., Dilbirligi, M., Sidhu, D., Erayman, M., Sandhu, D., Bondareva, S., Chao, S., Lazo, G.R., Anderson, O.D., Miftahudin, Gustafson, J.P., Echalier, B., Qi, L.L., Gill, B.S., Akhunov, E.D., Dvorak, J., Linkiewicz, A.M., Ratnasiri, A., Dubcovsky, J., Bermudez-Kandianis, C.E., Greene, R.A., Sorrells, M.E., Conley, E.J., Anderson, J.A., Peng, J.H., Lapitan, N.L.V., Hossain, K.G., Kalavacharla, V., Kianian, S.F., Pathan, M.S., Nguyen, H.T., Endo, T.R., Close, T.J., McGuire, P.E., Qualset, C.O., Gill, K.S., 2004. Deletion Mapping of Homoeologous Group 6-Specific Wheat Expressed Sequence Tags. Genetics 168, 677–686. doi:10.1534/genetics.104.034843

Richards, A.J., 1997. Plant Breeding Systems. Garland Science.

Riera-Lizarazu, O., Vales, M.I., Ananiev, E.V., Rines, H.W., Phillips, R.L., 2000. Production and Characterization of Maize Chromosome 9 Radiation Hybrids Derived From an Oat-Maize Addition Line. Genetics 156, 327–339.

Riera-Lizarazu, O., Leonard, J.M., Tiwari, V.K., Kianian, S.F., 2010. A Method to Produce Radiation Hybrids for the D-Genome Chromosomes of Wheat (*Triticum aestivum* L.). Cytogenetic and Genome Research 129, 234–240. doi:10.1159/000312723

Röder, M.S., Korzun, V., Wendehake, K., Plaschke, J., Tixier, M.H., Leroy, P., Ganal, M.W., 1998. A microsatellite map of wheat. Genetics 149, 2007–2023.

Saghai-Maroof, M.A., Soliman, K.M., Jorgensen, R.A., Allard, R.W., 1984. Ribosomal DNA spacer-length polymorphisms in barley: Mendelian inheritance, chromosomal location, and population dynamics. Proceedings of the National Academy of Sciences 81, 8014–8018.

Saintenac, C., Falque, M., Martin, O.C., Paux, E., Feuillet, C., Sourdille, P., 2009. Detailed Recombination Studies Along Chromosome 3B Provide New Insights on Crossover Distribution in Wheat (*Triticum aestivum* L.). Genetics 181, 393–403. doi:10.1534/genetics.108.097469

Sakai, K., Nasuda, S., Sato, K., Endo, T.R., 2009. Dissection of barley chromosome 3H in common wheat and a comparison of 3H physical and genetic maps. Genes & Genetic Systems 84, 25–34. doi:http://doi.org/10.1266/ggs.84.25

Salse, J., Bolot, S., Throude, M., Jouffe, V., Piegu, B., Quraishi, U.M., Calcagno, T., Cooke, R., Delseny, M., Feuillet, C., 2008. Identification and Characterization of Shared Duplications between Rice and Wheat Provide New Insight into Grass Genome Evolution. Plant Cell 20, 11–24. doi:10.1105/tpc.107.056309

Salvi, S., Tuberosa, R., 2005. To clone or not to clone plant QTLs: present and future challenges. Trends in Plant Science 10, 297–304. doi:10.1016/j.tplants.2005.04.008

Schroeder, H.W., Christensen, J.J., 1963. Factors affecting resistance of wheat to scab caused by *Gibberella zeae*. Phytopathology 53, 831–838.

Schuelke, M., 2000. An economic method for the fluorescent labeling of PCR fragments. Nature biotechnology 18, 233–234. doi:10.1038/72708

Schweiger, W., Steiner, B., Ametz, C., Siegwart, G., Wiesenberger, G., Berthiller, F., Lemmens, M., Jia, H., Adam, G., Muehlbauer, G.J., Kreil, D.P., Buerstmayr, H., 2013. Transcriptomic characterization of two major Fusarium resistance quantitative trait loci (QTLs), *Fhb1* and *Qfhs.ifa-5A*, identifies novel candidate genes. Molecular Plant Pathology 14, 772–785. doi:10.1111/mpp.12048

Sears, E.R., 1954. Aneuploids of common wheat. Mo. Agr. Exp. Sta. Res. Bull. 572, 1–58.

Sears, E.R., 1966. Nullisomic-tetrasomic combinations in hexaploid wheat, in: Chromosome Manipulations and Plant Genetics. p. pp 29-45. doi:10.1007/978-1-4899-6561-5

Sears, E.R., Sears, L.M., 1978. The telocentric chromosomes of common wheat, in: Proceedings of the 5th International Wheat Genetics Symposium. Indian Society for Genetics and Plant Breeding New Delhi, pp. 389–407.

Shirley, B.W., Hanley, S., Goodman, H.M., 1992. Effects of ionizing radiation on a plant genome: analysis of two Arabidopsis transparent testa mutations. The Plant Cell 4, 333–347.

Somers, D.J., Fedak, G., Savard, M., 2003. Molecular mapping of novel genes controlling Fusarium head blight resistance and deoxynivalenol accumulation in spring wheat. Genome 46, 555–564.

Somers, D.J., Isaac, P., 2004. SSRs from the Wheat Microsatellite Consortium [WWW Document]. URL http://wheat.pw.usda.gov/ggpages/SSR/WMC/ (accessed 5.27.16).

Somers, D.J., Isaac, P., Edwards, K., 2004. A high-density microsatellite consensus map for bread wheat (*Triticum aestivum* L.). Theoretical and Applied Genetics 109, 1105–1114. doi:10.1007/s00122-004-1740-7

Sorrells, M.E., Gustafson, J.P., Somers, D., Chao, S., Benscher, D., Guedira-Brown, G., Huttner, E., Kilian, A., McGuire, P.E., Ross, K., Tanaka, J., Wenzl, P., Williams, K., Qualset, C.O., Van Deynze, A., 2011. Reconstruction of the Synthetic W7984 × Opata M85 wheat reference population. Genome 54, 875–882. doi:10.1139/g11-054

Sourdille, P., Guyomarc'h, H., Baron, C., Gandon, B., Chiquet, V., Artiguenave, F., Edwards, K., Foisset, N., Dufour, P., 2001. Improvement of the genetic maps of wheat using new microsatellite markers. Plant & animal genome IX, final abstracts guide. Applied Biosystems Press, Foster City, Calif., 167.

Sturtevant, A.H., 1913. The linear arrangement of six sex-linked factors in Drosophila, as shown by their mode of association. Journal of experimental zoology 14, 43–59.

Tiwari, V.K., Riera-Lizarazu, O., Gunn, H.L., Lopez, K., Iqbal, M.J., Kianian, S.F., Leonard, J.M., 2012. Endosperm Tolerance of Paternal Aneuploidy Allows Radiation Hybrid Mapping of the Wheat D-Genome and a Measure of γ Ray-Induced Chromosome Breaks. PLoS ONE 7, e48815. doi:10.1371/journal.pone.0048815

Tiwari, V.K., Heesacker, A., Riera-Lizarazu, O., Gunn, H., Wang, S., Wang, Y., Gu, Y.Q., Paux, E., Koo, D.-H., Kumar, A., Luo, M.-C., Lazo, G., Zemetra, R., Akhunov, E., Friebe, B., Poland, J., Gill, B.S., Kianian, S., Leonard, J.M., 2016. A whole-genome, radiation hybrid mapping resource of hexaploid wheat. The Plant Journal 86, 195–207. doi:10.1111/tpj.13153

Van Vactor, D., Krantz, D.E., Reinke, R., Lawrence Zipursky, S., 1988. Analysis of mutants in chaoptin, a photoreceptor cell-specific glycoprotein in Drosophila, reveals its role in cellular morphogenesis. Cell 52, 281–290. doi:10.1016/0092-8674(88)90517-X

Vizir, I.Y., Mulligan, B.J., 1999. Genetics of gamma-irradiation-induced mutations in *Arabidopsis thaliana*: large chromosomal deletions can be rescued through the fertilization of diploid eggs. Journal of Heredity 90, 412–417. doi:10.1093/jhered/90.3.412

Vogel, J.P., Garvin, D.F., Mockler, T.C., Schmutz, J., Rokhsar, D., Bevan, M.W., Barry, K., Lucas, S., Harmon-Smith, M., Lail, K., Tice, H., Schmutz (Leader), J., Grimwood, J., McKenzie, N., Bevan, M.W., Huo, N., Gu, Y.Q., Lazo, G.R., Anderson, O.D., Vogel (Leader), J.P., You, F.M., Luo, M.-C., Dvorak, J., Wright, J., Febrer, M., Bevan, M.W., Idziak, D., Hasterok, R., Garvin, D.F., Lindquist, E., Wang, M., Fox, S.E., Priest, H.D.,

Filichkin, S.A., Givan, S.A., Bryant, D.W., Chang, J.H., Mockler (Leader), T.C., Wu, H., Wu, W., Hsia, A.-P., Schnable, P.S., Kalyanaraman, A., Barbazuk, B., Michael, T.P., Hazen, S.P., Bragg, J.N., Laudencia-Chingcuanco, D., Vogel, J.P., Garvin, D.F., Weng, Y., McKenzie, N., Bevan, M.W., Haberer, G., Spannagl, M., Mayer (Leader), K., Rattei, T., Mitros, T., Rokhsar, D., Lee, S.-J., Rose, J.K.C., Mueller, L.A., York, T.L., Wicker (Leader), T., Buchmann, J.P., Tanskanen, J., Schulman (Leader), A.H., Gundlach, H., Wright, J., Bevan, M., Costa de Oliveira, A., da C. Maia, L., Belknap, W., Gu, Y.Q., Jiang, N., Lai, J., Zhu, L., Ma, J., Sun, C., Pritham, E., Salse (Leader), J., Murat, F., Abrouk, M., Haberer, G., Spannagl, M., Mayer, K., Bruggmann, R., Messing, J., You, F.M., Luo, M.-C., Dvorak, J., Fahlgren, N., Fox, S.E., Sullivan, C.M., Mockler, T.C., Carrington, J.C., Chapman, E.J., May, G.D., Zhai, J., Ganssmann, M., Guna Ranjan Gurazada, S., German, M., Meyers, B.C., Green (Leader), P.J., Bragg, J.N., Tyler, L., Wu, J., Gu, Y.Q., Lazo, G.R., Laudencia-Chingcuanco, D., Thomson, J., Vogel (Leader), J.P., Hazen, S.P., Chen, S., Scheller, H.V., Harholt, J., Ulvskov, P., Fox, S.E., Filichkin, S.A., Fahlgren, N., Kimbrel, J.A., Chang, J.H., Sullivan, C.M., Chapman, E.J., Carrington, J.C., Mockler, T.C., Bartley, L.E., Cao, P., Jung, K.-H., Sharma, M.K., Vega-Sanchez, M., Ronald, P., Dardick, C.D., De Bodt, S., Verelst, W., Inzé, D., Heese, M., Schnittger, A., Yang, X., Kalluri, U.C., Tuskan, G.A., Hua, Z., Vierstra, R.D., Garvin, D.F., Cui, Y., Ouyang, S., Sun, Q., Liu, Z., Yilmaz, A., Grotewold, E., Sibout, R., Hematy, K., Mouille, G., Höfte, H., Michael, T., Pelloux, J., O'Connor, D., Schnable, J., Rowe, S., Harmon, F., Cass, C.L., Sedbrook, J.C., Byrne, M.E., Walsh, S., Higgins, J., Bevan, M., Li, P., Brutnell, T., Unver, T., Budak, H., Belcram, H., Charles, M., Chalhoub, B., Baxter, I., 2010. Genome sequencing and analysis of the model grass *Brachypodium distachyon*. Nature 463, 763–768. doi:10.1038/nature08747

Wang, S., Wong, D., Forrest, K., Allen, A., Chao, S., Huang, B.E., Maccaferri, M., Salvi, S., Milner, S.G., Cattivelli, L., Mastrangelo, A.M., Whan, A., Stephen, S., Barker, G., Wieseke, R., Plieske, J., International Wheat Genome Sequencing Consortium, Lillemo, M., Mather, D., Appels, R., Dolferus, R., Brown-Guedira, G., Korol, A., Akhunova, A.R., Feuillet, C., Salse, J., Morgante, M., Pozniak, C., Luo, M.-C., Dvorak, J., Morell, M., Dubcovsky, J., Ganal, M., Tuberosa, R., Lawley, C., Mikoulitch, I., Cavanagh, C., Edwards, K.J., Hayden, M., Akhunov, E., 2014. Characterization of polyploid wheat genomic diversity using a high-density 90 000 single nucleotide polymorphism array. Plant Biotechnology Journal 12, 787–796. doi:10.1111/pbi.12183

Wardrop, J., Fuller, J., Powell, W., Machray, G.C., 2004. Exploiting plant somatic radiation hybrids for physical mapping of expressed sequence tags. Theoretical and Applied Genetics 108, 343–348. doi:10.1007/s00122-003-1434-6

Wardrop, J., Snape, J., Powell, W., Machray, G.C., 2002. Constructing plant radiation hybrid panels. The Plant Journal 31, 223–228. doi:10.1046/j.1365-313X.2002.01351.x

Werner, J.E., Endo, T.R., Gill, B.S., 1992. Toward a Cytogenetically Based Physical Map of the Wheat Genome. Proceedings of the National Academy of Sciences of the United States of America 89, 11307–11311.

Womack, J.E., Johnson, J.S., Owens, E.K., Rexroad, C.E., Schläpfer, J., Yang, Y.-P., 1997. A whole-genome radiation hybrid panel for bovine gene mapping. Mammalian Genome 8, 854–856.

Xue, S., Xu, F., Tang, M., Zhou, Y., Li, G., An, X., Lin, F., Xu, H., Jia, H., Zhang, L., Kong, Z., Ma, Z., 2011. Precise mapping *Fhb5*, a major QTL conditioning resistance to Fusarium infection in bread wheat (*Triticum aestivum* L.). Theoretical and Applied Genetics 123, 1055–1063. doi:10.1007/s00122-011-1647-z

Xue, S., Zhang, Z., Lin, F., Kong, Z., Cao, Y., Li, C., Yi, H., Mei, M., Zhu, H., Wu, J., Xu, H., Zhao, D., Tian, D., Zhang, C., Ma, Z., 2008. A high-density intervarietal map of the

wheat genome enriched with markers derived from expressed sequence tags. Theoretical and Applied Genetics 117, 181–189. doi:10.1007/s00122-008-0764-9

Yamano, S., Tsujimoto, H., Endo, T.R., Nasuda, S., 2010. Radiation mutants for mapping genes and markers in pericentromeric region of chromosome 3B of Norin 26 wheat. Wheat Inf Serv 11–13.

You, Y., Bergstrom, R., Klemm, M., Lederman, B., Nelson, H., Ticknor, C., Jaenisch, R., Schimenti, J., 1997. Chromosomal deletion complexes in mice by radiation of embryonic stem cells. Nature Genetics 15, 285–288. doi:10.1038/ng0397-285

Zhou, C., Xia, G., Zhi, D., Chen, Y., 2006. Genetic characterization of asymmetric somatic hybrids between *Bupleurum scorzonerifolium* Willd and *Triticum aestivum* L.: potential application to the study of the wheat genome. Planta 223, 714–724. doi:10.1007/s00425-005-0127-6

Zhou, C., Dong, W., Han, L., Wei, J., Jia, L., Tan, Y., Zhi, D., Wang, Z.-Y., Xia, G., 2012. Construction of Whole Genome Radiation Hybrid Panels and Map of Chromosome 5A of Wheat Using Asymmetric Somatic Hybridization. PLoS ONE 7, e40214. doi:10.1371/journal.pone.0040214